



Department of Information Science and Technology

# Performance analysis of Massive MIMO receivers

Daniel Filipe Sobral Fernandes

A Dissertation presented in partial fulfillment of the Requirements  
for the Degree of  
**Master in Telecommunications and Computer Engineering**

## **Supervisor**

Prof. Dr. Francisco António Bucho Cercas, Full Professor  
ISCTE-IUL

## **Co-Supervisor**

Prof. Dr. Rui Miguel Henriques Dias Morgado Dinis, Associate  
Professor  
FCT-UNL

June 2017



# *Resumo*

Atualmente, sente-se um aumento exponencial nos dispositivos wireless. De modo a permitir uma boa experiência por parte dos utilizadores é fundamental que a próxima geração de comunicações móveis (5G) assegure fiabilidade nas ligações, uma elevada taxa de transferência de dados e baixa latência.

Uma maneira de elevar a taxa de transferência de dados é utilizar sistemas massive Multiple-Input, Multiple-Output (MIMO), ou seja, sistemas com múltiplas antenas a emitir e múltiplas antenas a receber permitindo assim diversidade espacial. Nestes sistemas, para aumentar a bateria dos dispositivos é preferível usar no uplink a modulação Single-Carrier with Frequency-Domain Equalization pois esta modulação reduz a complexidade no emissor transferindo-a para o receptor, neste caso na Base Station, onde isso é bastante aceitável.

Esta dissertação estuda o desempenho dos recetores dos sistemas massive MIMO, comparando o desempenho alcançado com o desempenho do Matched Filter Bound (MFB). O recetor Iterative Block Decision-Feedback Equalizer (IB-DFE) apresenta um desempenho muito semelhante ao do MFB no entanto, o algoritmo do receptor inverte matrizes, o que nos sistemas em estudo, onde o tamanho das matrizes é elevado, se reflecte no aumento da complexidade das operações associadas. Deste modo, é importante que sejam utilizados recetores de baixa complexidade tal como o Maximal-Ratio Combining (MRC) ou o Equal Gain Combining.

Esta dissertação propõe um recetor simples que combina um recetor IB-DFE com um recetor MRC, criando desde modo um recetor de baixa complexidade e com excelente desempenho.

**Palavras-chave:** SC-FDE, IB-DFE, Zero Forcing, MRC, EGC, MIMO, Massive MIMO.



# *Abstract*

We face now an exponential increase in wireless devices and to allow good user experience, it is imperative that the next generation of mobile (5G) communications ensures reliable connections, high data transfer rates and low latency.

One way to increase the data transfer rate is to use massive Multiple-Input, Multiple-Output (MIMO) systems, that is, systems with multiple antennas to emit and multiple antennas to receive thus allowing spatial diversity. In these systems, to increase the battery life of the devices it is preferable to use the Single-Carrier with Frequency-Domain Equalization modulation in the uplink as this modulation reduces the complexity in the emitter, transferring it to the receiver, in this case the Base Station, where it is quite acceptable.

This dissertation studies the performance of massive MIMO receiver systems, comparing it to the performance achieved with the Matched Filter Bound (MFB). The Iterative Block Decision-Feedback Equalizer (IB-DFE) receiver presents a very similar performance to the MFB, however, the algorithm requires matrix inversions, which in the systems under study, where the size of the matrix is high, implies an increase of the associated operations. Thus it is very important that low complexity receivers, such as the Maximal-Ratio Combining (MRC) or Equal Gain Combining are used.

In this dissertation, a simple receiver is proposed combining the IB-DFE receiver with the MRC receiver, thus creating a low complexity receiver with excellent performance.

**Keywords:** SC-FDE, IB-DFE, Zero Forcing, MRC, EGC, MIMO, Massive MIMO.



# *Acknowledgements*

First of all I would like to thank my supervisor, Prof. Dr. Francisco Cercas, for his constant support, guidance, motivation and encouragement during this work. Likewise, I would also like to thank my co-supervisor, Prof. Dr. Rui Dinis, for his motivation, encouragement and willingness to clarify all the scientific doubts encountered throughout the research work.

Secondly, I would like to thank my parents, my sister, my grandparents and all my family for all the support and dedication given over the years. I also want to thank Susan for her contributions with linguistic advices.

This work would have not been possible without the constant support, motivation, company and encouragement of my friends Inês, Pedro, Rodrigo, Miriam, João, André and all the other friends and colleagues. My colleagues and friends of the Portuguese Red Cross - Delegation of Setúbal also supported me at this stage.

My final thanks go to the undoubted support promoted by Fundação para a Ciência e Tecnologia in the context of research projects PEst-OE / EEI / LA0008 / 2013 and UID / EEA / 50008/2013 - MM5G.





# Contents

<b>Resumo</b>	<b>iii</b>
<b>Abstract</b>	<b>v</b>
<b>Acknowledgements</b>	<b>vii</b>
<b>List of Figures</b>	<b>xi</b>
<b>List of Acronyms</b>	<b>xiii</b>
<b>List of Symbols</b>	<b>xv</b>
<b>1 Introduction</b>	<b>1</b>
1.1 Motivation and Scope . . . . .	1
1.2 Objectives . . . . .	3
1.3 Thesis Organization . . . . .	3
1.4 Notation and Simulations Aspects . . . . .	4
<b>2 State of the Art</b>	<b>5</b>
2.1 Evolution to 5G . . . . .	5
2.2 Block Transmission Techniques . . . . .	6
2.2.1 Multicarrier versus Single-Carrier modulations . . . . .	6
2.2.2 OFDM . . . . .	7
2.2.3 SC-FDE . . . . .	9
2.2.4 IB-FDE . . . . .	11
2.3 Multiple-Input, Multiple-Output systems . . . . .	14
2.3.1 MIMO . . . . .	14
2.3.2 Massive MIMO . . . . .	15
<b>3 Receivers for Massive MIMO</b>	<b>17</b>
3.1 IB-DFE for MIMO systems . . . . .	17
3.2 Zero Forcing . . . . .	22
3.3 Linear MRC . . . . .	25
3.4 Linear EGC . . . . .	26
<b>4 Low complexity receivers for Massive MIMO systems</b>	<b>31</b>
4.1 Iterative MRC . . . . .	31

4.2	Iterative EGC . . . . .	35
4.3	Comparison between receivers . . . . .	38
4.4	The proposed receiver . . . . .	43
4.5	Results . . . . .	45
<b>5</b>	<b>Conclusions and Future Work</b>	<b>51</b>
5.1	Conclusions . . . . .	51
5.2	Future Work . . . . .	52
	<b>Appendices</b>	<b>55</b>
	<b>A Publications</b>	<b>57</b>
	<b>Bibliography</b>	<b>71</b>

# List of Figures

2.1	OFDM transmission chain. . . . .	8
2.2	SC-FDE transmission chain. . . . .	9
2.3	BER performance comparison for SC-FDE with ZF and MMSE equalization. . . . .	11
2.4	IB-DFE receiver structure. . . . .	12
2.5	BER performance for an IB-DFE receiver with four iterations. . . . .	13
3.1	MIMO system. . . . .	18
3.2	MIMO IB-DFE receiver structure. . . . .	19
3.3	BER performance for IB-DFE receiver with $P = 2$ MTs and $R = 6$ BSs. . . . .	20
3.4	BER performance for IB-DFE receiver with $P = 60$ MTs and $R = 180$ BSs. . . . .	21
3.5	BER performance for IB-DFE receiver with $P = 60$ MTs and $R = 360$ BSs. . . . .	21
3.6	BER performance for IB-DFE and ZF receivers with $P = 2$ MTs and $R = 6$ BSs. . . . .	23
3.7	BER performance for IB-DFE and ZF receivers with $P = 60$ MTs and $R = 180$ BSs. . . . .	24
3.8	BER performance for IB-DFE and ZF receivers with $P = 60$ MTs and $R = 360$ BSs. . . . .	24
3.9	Massive MIMO receiver and equalization for linear MRC. . . . .	25
3.10	BER performance for MRC and EGC receivers with $P = 2$ MTs and different values of $R$ BSs. . . . .	27
3.11	BER performance for MRC and EGC receivers with $P = 60$ MTs and different values of $R$ BSs. . . . .	28
3.12	BER performance for MRC and EGC receivers with $P = 120$ MTs and different values of $R$ BSs. . . . .	28
4.1	Massive MIMO receiver and equalization for iterative MRC. . . . .	32
4.2	BER performance for MRC receiver with $P = 2$ MTs and $R = 6$ BSs. . . . .	33
4.3	BER performance for MRC receiver with $P = 60$ MTs and $R = 180$ BSs. . . . .	34
4.4	BER performance for MRC receiver with $P = 60$ MTs and $R = 360$ BSs. . . . .	34
4.5	BER performance for EGC receiver with $P = 2$ MTs and $R = 6$ BSs. . . . .	36

4.6	BER performance for EGC receiver with $P = 60$ MTs and $R = 180$ BSs. . . . .	37
4.7	BER performance for EGC receiver with $P = 60$ MTs and $R = 360$ BSs. . . . .	37
4.8	BER performance for IB-DFE and MRC receivers with $P = 60$ MTs and $R = 180$ BSs. . . . .	39
4.9	BER performance for IB-DFE and MRC receivers with $P = 60$ MTs and $R = 360$ BSs. . . . .	39
4.10	BER performance for IB-DFE and EGC receivers with $P = 60$ MTs and $R = 180$ BSs. . . . .	40
4.11	BER performance for IB-DFE and EGC receivers with $P = 60$ MTs and $R = 360$ BSs. . . . .	41
4.12	BER performance for MRC and EGC receivers with $P = 60$ MTs and $R = 180$ BSs. . . . .	42
4.13	BER performance for MRC and EGC receivers with $P = 60$ MTs and $R = 360$ BSs. . . . .	42
4.14	Proposed receiver. . . . .	43
4.15	BER performance for the proposed receiver with $P = 2$ MTs and $R = 6$ BSs. . . . .	46
4.16	BER performance for the proposed receiver with $P = 60$ MTs and $R = 180$ BSs. . . . .	46
4.17	BER performance for the proposed receiver with $P = 120$ MTs and $R = 360$ BSs. . . . .	47
4.18	BER performance for the proposed receiver with $P = 120$ MTs and $R = 480$ BSs. . . . .	48
4.19	BER performance for the proposed receiver with $P = 60$ MTs and $R = 360$ BSs. . . . .	49

# List of Acronyms

5G	5G
BER	Bit Error Rate
BS	Base Station
CP	Cycle Prefix
DFE	Decision-Feedback Equalizer
EGC	Equal Gain Combining
FDE	Frequency Domain Equalization
FDM	Frequency Division Multiplexing
FFT	Fast Fourier Transform
FT	Fourier Transform
IB-DFE	Iterative Block Decision-Feedback Equalizer
IFFT	Inverse Fast Fourier Transform
IoT	Internet of Things
ISI	Inter-Symbol Interference
MC	Multicarrier
MFB	Matched Filter Bound
MIMO	Multiple-Input, Multiple-Output
MMSE	Minimum Mean Square Error
mmW	millimeter Wave
MRC	Maximal-Ratio Combining
MT	Mobile Terminal

OFDM	Orthogonal Frequency-Division Multiplexing
PMEPR	Peak-to-Mean Envelope Power Ratio
QPSK	Quaternary Phase Shift Keying
SC	Single-Carrier
SC-FDE	Single-Carrier with Frequency-Domain Equalization
SINR	Signal to Interference-plus-Noise Ratio
SISO	Single-Input, Single-Output
SNR	Signal-to-Noise Ratio
SVD	Singular Value Decomposition
ZF	Zero Forcing

# List of Symbols

$B_k$	feedback equalizer coefficient for the $k^{th}$ frequency
$B_{k,p}$	feedback equalizer coefficient for the $k^{th}$ frequency and the $p^{th}$ user
$E_b$	average bit energy
$F$	sub-carrier separation
$F_k$	feedforward equalizer coefficient for the $k^{th}$ frequency
$F_{k,p}$	feedforward equalizer coefficient for the $k^{th}$ frequency and the $p^{th}$ user
$H_k$	overall channel frequency response for the $k^{th}$ frequency
$N$	number of samples/sub-carriers
$N_G$	number of guard samples
$N_k$	channel noise for the $k^{th}$ frequency
$N_0$	noise power spectral density (unilateral)
$P$	number of users
$R$	number of receiving antennas
$R(f)$	Fourier transform of $r(t)$
$S(f)$	frequency-domain signal
$S_k$	$k^{th}$ frequency-domain data symbol
$T$	duration of the useful part of the block
$T_B$	block duration
$T_s$	symbol duration
$Y_k$	received sample for the $k^{th}$ frequency

$\Psi$	diagonal matrix with normalization parameter
$\alpha$	scale factor associated to the nonlinear operation
$\mathbf{A}$	matrix diagonal where elements have absolute value of 1 and phase identical to the corresponding element of $\mathbf{H}_k$
$\mathbf{U}_k$	unitary matrix where left column is singular value of $\mathbf{H}_k$
$\mathbf{V}_k$	unitary matrix where right column is singular value of $\mathbf{H}_k$
$\Delta_k$	error terms matrix for the $k^{th}$ frequency
$\Sigma_k$	matrix diagonal where elements have singular values of $\mathbf{H}_k$
$f$	frequency variable
$i$	iteration index
$k$	frequency index
$n$	time index
$p$	user index
$r$	receiving antenna index
$r(t)$	rectangular impulse; shapping impulse
$s(t)$	time-domain signal
$s_n$	$n^{th}$ time-domain data symbol
$t$	time variable
$y_n$	$n^{th}$ time-domain received sample
$\bar{S}_{k,p}$	"soft decision" for the $k^{th}$ frequency-domain data symbol of the $p^{th}$ user
$\bar{s}_{n,p}$	"soft decision" of the $n^{th}$ time-domain data symbol of the $p^{th}$ user
$\hat{S}_k$	"hard decision" for the $k^{th}$ frequency-domain data symbol
$\hat{s}_n$	"hard decision" of the $n^{th}$ time-domain data symbol
$\rho$	correlation coefficient
$\tilde{S}_k$	estimate for the $k^{th}$ frequency-domain data symbol
$\tilde{S}_{k,p}$	estimate for the $k^{th}$ frequency and the $p^{th}$ user
$\tilde{s}_n$	sample estimate for the $n^{th}$ time-domain data symbol
$\mathbf{P}$	correlation coefficients matrix



# Chapter 1

## Introduction

### 1.1 Motivation and Scope

Communication methods have been around for several centuries. The need for humanity to communicate at long distances dates almost as back as humanity itself, with rudimentary methods dating back to that era. Later in the **19<sup>th</sup>** century, the technological revolution opened the doors to the introduction of new communication methods and allowed Alexander Bell and Elisha Gray to create the first cable telephone in 1876. Since then, the evolution in this area has been remarkable. We are now in the wireless era, where electromagnetism and a simple set of equations known as Maxwell's equations built the foundation of global wireless communications. With the recent proliferation and evolution of wireless devices and their use, the content consumed by final users is increasing and getting even more complex with the number of users growing exponentially. For this reasons, the telecommunications area is in constant innovation and evolution. We are now moving towards considerable progress: the **5<sup>th</sup>** generation network of mobile communication.

The next generation network of mobile communications is the natural development of mobile telecommunication standards due to the exponential growth of the wirelesses traffic volume. This growth results, in part, from the demand of entertainment and news in real-time. This will rise exponentially with the advent

of Internet of Things (IoT), where all our gadgets and machines can be connected and will communicate. As we can see, 5G must support diverse specifications like reliability, lower latency and high data rates. Devices should also present low complexity for an increased battery life [1].

A possible solution to achieve the 5G specifications is to use massive MIMO (Multiple-Input, Multiple-Output) systems, where multiple transmitting and receiving antennas are used. This technology uses the base station not only for the uplink (transmission from the Mobile Terminal (MT) to the Base Station (BS)) but also in downlink (transmission from the BS to the MT) with the channel knowledge, so it is possible to offer spatial multiplexing [2]. In this work the major concern is related to the uplink scenario.

Conventional MIMO receivers have a complex hardware implementation related with matrix inversions and a large energy consumption in order to process the received signal [3]. To achieve the objectives of 5G, the massive MIMO schemes can be combined with Single-Carrier with Frequency-Domain Equalization (SC-FDE), as the channels are highly selective in the frequency.

Iterative receivers, such as the Iterative Block Decision-Feedback Equalizer (IB-DFE), have an excellent performance with MIMO [4] but, by increasing the number of transmit antennas, the size of matrixes grows, raising the complexity of matrix inversions. For this reason, the use of this type of receivers and the linear receiver Zero Forcing (ZF) is very limited.

Although receivers that do not require matrix inversions already exist, like the MRC (Maximal-Ratio Combining) and Equal Gain Combining (EGC), the performance of these receivers does not reach the performance of an iterative receiver, although its complexity is much lower.

All the information stated before leads us to a great issue of research which is the main goal of this dissertation: Is it possible to design a receiver with a similar performance to the iterative receiver while maintaining the complexity of receivers that don't require matrix inversions?

## 1.2 Objectives

Throughout this work, the performance of the receivers that do not require matrix inversion will then be studied using theoretical and simulation tools. Then, the obtained results will be analyzed and compared with the existing state of the art published in recent literature. This, in term, will fulfill the challenge the question presented earlier.

Another objective of this work is to develop these receivers so that they can be used in 5G technology.

Finally, the obtained results will be published in international conferences on Telecommunications.

## 1.3 Thesis Organization

After this first introductory chapter, chapter 2 begins with the evolution of telecommunication systems up to date, followed by an explanation of block transmission techniques. In this case, the differences between multicarrier and single-carrier modulations are first explained and then a more detailed explanation is given for Orthogonal Frequency-Division Multiplexing (OFDM) modulation and the SC-FDE modulation. In these explanations, the transmission schemes are presented and their differences are highlighted. In the case of the SC-FDE modulation, the IB-DFE receiver and its performance is presented. Finally, the chapter introduces the concept of MIMO and massive MIMO systems.

In chapter 3, the extension of the IB-DFE receiver for massive MIMO systems is presented. In this case, the scenario under study and the receiver scheme are explained. Subsequently, the performance achieved by this receiver for different case studies, where the number of emitting and receiving antennas varies, is presented. The ZF receiver and its performance is also presented. Finally, the linear version of the low complexity receivers MRC and EGC is explained.

In chapter 4, the low complexity linear receivers presented earlier are again brought to discussion together with the achieved performance, in this case in its iterative version. In this chapter, a comparison is made between all the iterative receivers presented previously. Finally a receiver of low complexity is proposed and analysed that combines two different receivers.

Finally in chapter 5 the conclusions of the work accomplished and the perspectives for the future work are highlighted.

## 1.4 Notation and Simulations Aspects

Throughout this dissertation, the following notation is adopted: bold upper case letters denote matrices or vectors;  $\mathbf{I}_N$  denote the  $N \times N$  identity matrix;  $(\cdot)^T$ ,  $(\cdot)^*$ ,  $(\cdot)^H$ ,  $diag(\cdot)$  denote the transpose, complex conjugate, hermitian (complex conjugate transpose) and diagonal matrices, respectively;  $[\mathbf{X}]_{n,m}$  denotes the element of line  $n$  and column  $m$  of matrix  $\mathbf{X}$ .  $\mathbb{E}[\cdot]$  denotes expectation.

In general, upper case letters denote frequency-domain variables and lower case letters denote time-domain variables;  $(\tilde{\cdot})$ ,  $(\hat{\cdot})$  and  $(\bar{\cdot})$  denote sample estimates, "hard decision" estimate and "soft decision" estimates, respectively.

The performance results presented in this dissertation were obtained by Monte Carlo simulations using the MatLab software environment.

As the accuracy achieved by the Monte Carlo simulations depends on the number of simulated blocks transmitted, the simulations were conducted with data blocks of  $N = 256$  Quaternary Phase Shift Keying (QPSK) symbols per block. Every channel has 100 slots, symbol-spaced, equal-power multipath components.

In all cases it is assumed perfect synchronism between the transmitted blocks associated to the different users and perfect channel estimation.

# Chapter 2

## State of the Art

This chapter deals with literature review of the most important aspects related to the work herein developed. It is divided as follows: Section 2.1 presents the main reasons for the development of the 5<sup>th</sup> generation network of mobile communication. Section 2.2 describes the OFDM and SC-FDE modulations showing their transmission chain diagrams. The IB-DFE concept is also presented in this section. Finally, section 2.3 presents the theoretical concepts of MIMO and massive MIMO.

### 2.1 Evolution to 5G

In 1981, in Norway, it was implemented the first communication system (the first generation) that allowed voice transmission using analog modulation. The search for more advanced voice services and the exchange of small messages urged the need to evolve to the second generation, a digital generation. In the 1980s, the third generation began to be planned, which would bring the Internet to the mobile devices of users anywhere. In order to allow users new levels of experience and multi-service capability, the need to move to the fourth generation has arisen [5].

The requirements currently imposed, such as low latency and high bit rates, lead to the concept of 5G. With the passage from the fourth generation to the fifth

generation the spectral efficiency will increase as well as the data rate which may increase up to  $1000\times$ . According to [6] this increase of  $1000\times$  is due to the extreme densification of active nodes, the use of millimeter Wave (mmW) technology, that allows the establishment of wireless connections with a high data transfer [7] and, finally, the use of MIMO.

## 2.2 Block Transmission Techniques

This section deals with several block transmission techniques. Initially the Single-Carrier (SC) modulation, where the information is transmitted in the time-domain is discussed. Subsequently the modulations where information is transmitted in the frequency-domain are presented: the Multicarrier (MC) modulations.

### 2.2.1 Multicarrier versus Single-Carrier modulations

In a Single-Carrier modulation the energy associated with each symbol is distributed over the entire bandwidth. In the time-domain, the expression for the complex envelope of a  $N$ -symbol burst ( $N$  is considered an even value for reasons of simplicity) can be written as:

$$s(t) = \sum_{n=0}^{N-1} s_n r(t - nT_s), \quad (2.1)$$

where  $s_n$  is a complex coefficient corresponding to the  $n^{th}$  symbol determined from a certain constellation (e.g., a QPSK constellation),  $T_s$  is the symbol duration and  $r(t)$  represents the transmitted impulse. The corresponding expression in the frequency-domain, represented in 2.2 is obtained by applying the Fourier Transform (FT).

$$S(f) = \mathcal{F}\{s(t)\} = \sum_{k=0}^{N-1} s_n R(f) e^{-j2\pi f n T_s}, \quad (2.2)$$

in which  $R(f)$  is the FT of  $r(t)$ . Thus the transmission band associated to each symbol  $s_n$  is the band occupied by  $R(f)$ .

Multicarrier modulations are characterized by the transmission of information in the frequency-domain according to the following expression:

$$S(f) = \sum_{k=0}^{N-1} S_k R(f - kF). \quad (2.3)$$

During the same time interval,  $T$ , the  $N$  symbols are distributed by  $N$  different sub-carriers. In expression 2.3,  $F = \frac{1}{T}$  represents the spacing between the sub-carriers and the  $S_k$  symbolizes the  $k^{\text{th}}$  symbol in the frequency-domain. Applying the inverse FT the following expression is obtained:

$$s(t) = \mathcal{F}^{-1}\{S(f)\} = \sum_{k=0}^{N-1} S_k r(t) e^{j2\pi k F t}. \quad (2.4)$$

Frequency Division Multiplexing (FDM) is the simplest multicarrier modulation where overlapping of sub-carriers does not occur.

In order for the impulses of  $r(t)$  to be orthogonal and thus to avoid ISI (Inter-Symbol Interference), the following condition must be met:

$$\int_{-\infty}^{+\infty} r(t - nT_s) r^*(t - n'T_s) dt = 0, n \neq n'. \quad (2.5)$$

For the case of multicarrier modulations the expression is analogous to 2.5:

$$\int_{-\infty}^{+\infty} R(f - kF) R^*(f - k'F) df = 0, k \neq k'. \quad (2.6)$$

## 2.2.2 OFDM

In the year of 1966, a multicarrier modulation was proposed, the Orthogonal Frequency-Division Multiplexing (OFDM) [8] in which the information is sent through  $N$  subcarriers, respecting the principles of orthogonality [9]. The spacing

between them is  $F \geq \frac{1}{T_B}$ , where  $T_B$  is the duration of an OFDM block, which is revealed in a total available bandwidth of  $N \times F$ . This type of modulation allows a higher spectral efficiency to be achieved when compared to FDM, since, due to orthogonality, the spectrum of the subcarriers may overlap [10].

The data is sent in the frequency-domain and has a size  $N$  of  $\{S_k; k = 0, 1, \dots, N-1\}$ , a block of  $N$  complex symbols, chosen from a selected constellation (e.g., QPSK constellation). After the data passes through the Inverse Fast Fourier Transform (IFFT), a Cycle Prefix (CP) of  $N_G$  samples is added at the beginning of each block of  $N$  IFFT coefficients. This prefix is a cycle extension, in the time domain, of the OFDM block. The transmitted block is  $\{s_n; n = -N_G, \dots, N-1\}$  with a time duration of  $N + N_G$ .

At the receiver end, after the CP is removed and the data block passes the Fast Fourier Transform (FFT) block, the samples  $\{Y_k; k = 0, 1, \dots, N-1\}$ , already in the frequency-domain, are subjected to Frequency Domain Equalization (FDE). After the FDE block, the samples,  $\tilde{s}_n$ , pass through a decision device yielding an estimated sample  $\hat{s}_n$ . The complete transmission chain is represented in Fig. 2.1.

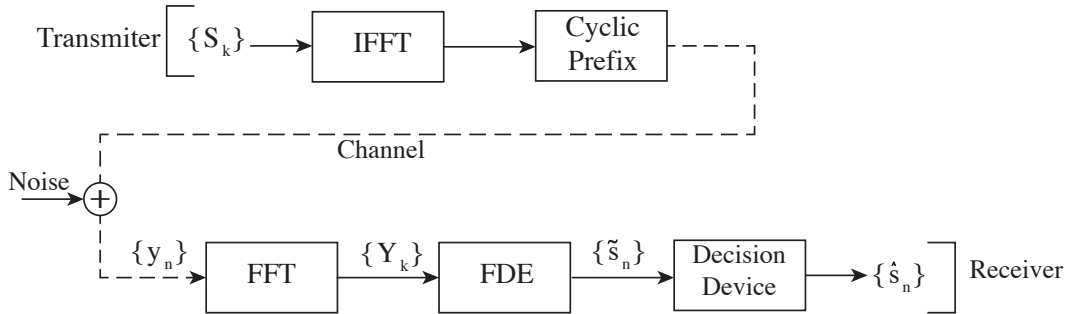


FIGURE 2.1: OFDM transmission chain.



### 2.2.3 SC-FDE

OFDM modulations are vulnerable to transmitter nonlinearities, especially those associated with power amplifiers since the OFDM scenario undergoes large envelope fluctuations and a high Peak-to-Mean Envelope Power Ratio (PMEPR) [11]. Therefore, this type of modulation should be used in downlink communications [12]. Since with SC-FDE modulations, the signals have low envelope fluctuations and the emitters have a high power efficiency, this type of modulation must be used in the MT, that is, in the uplink scenarios. This allows MTs to be cheap and to increase the life of batteries. However, the signals may suffer from high distortion which makes the transmission bandwidth larger than the channels's coherence bandwidth, thus increasing the complexity of the receivers [13].

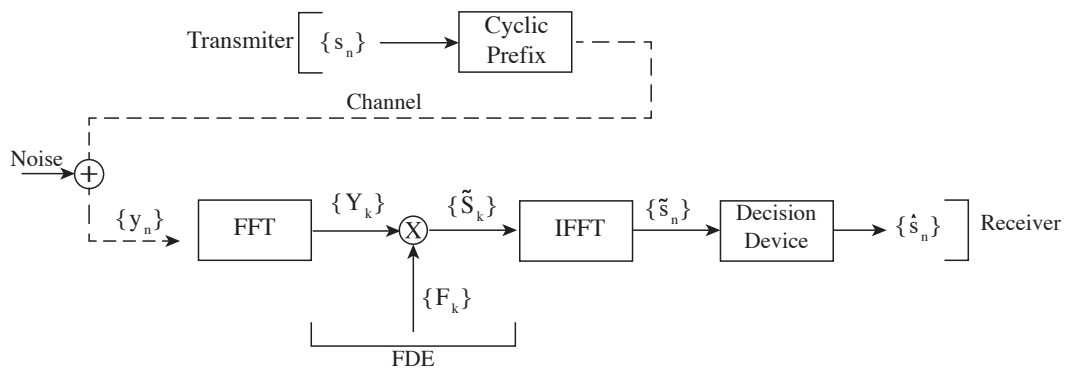


FIGURE 2.2: SC-FDE transmission chain.

In Fig. 2.2 the block transmission chain is represented for this type of modulation. The data is transmitted in blocks of  $N$  convenient modulated time-domain symbols  $\{s_n; n = 0, \dots, N - 1\}$ , where  $s_n$  is chosen according to a given mapping rule (e.g., QPSK constellation with Gray mapping). Before the blocks are transmitted, a CP is inserted, as explained in the preceding section, resulting in the following transmitted signal:  $\{s_n; n = -N_G, \dots, N - 1\}$ . At the receiver, the CP is withdrawn from the received data, obtaining the samples  $\{y_n; n = 0, \dots, N - 1\}$  in the time-domain. The  $y_n$  samples then continue through the transmission chain and pass the FFT block, which turns them into frequency-domain samples,

$\{Y_k; k = 0, \dots, N - 1\}$  where  $Y_k$  is characterized by the following expression:

$$Y_k = H_k S_k + N_k. \quad (2.7)$$

In equation 2.7,  $H_k$  represents the frequency channel response for the  $k^{th}$  subcarrier and  $N_k$  the Gaussian channel noise component, in the frequency-domain, for that subcarrier. After the equalizer, the frequency-domain samples  $\tilde{S}_k$  result in expression 2.8.

$$\tilde{S}_k = F_k Y_k. \quad (2.8)$$

$F_k$  represents the feedforward coefficient of the equalization process and can be defined according to the criterion ZF (expression 2.9) or Minimum Mean Square Error (MMSE) (expression 2.10).

$$F_k = \frac{1}{H_k} = \frac{H_k^*}{|H_k|^2} \quad (2.9)$$

$$F_k = \frac{H_k^*}{\frac{1}{SNR} + |H_k|^2} \quad (2.10)$$

As it is possible to verify, in the case of the equalizer ZF, the channel is completely inverted which can increase the noise in a frequency-selective channel, resulting in a decrease of the Signal-to-Noise Ratio (SNR). This problem can be overcome using the MMSE [14].

The Bit Error Rate (BER) performance in the scenarios of SC-FDE with ZF and MMSE equalization is presented in Fig. 2.3. In the case of the MMSE criterion, a better performance is achieved due to the fact that this criterion allows to minimize the combined effects of channel noise and ISI.

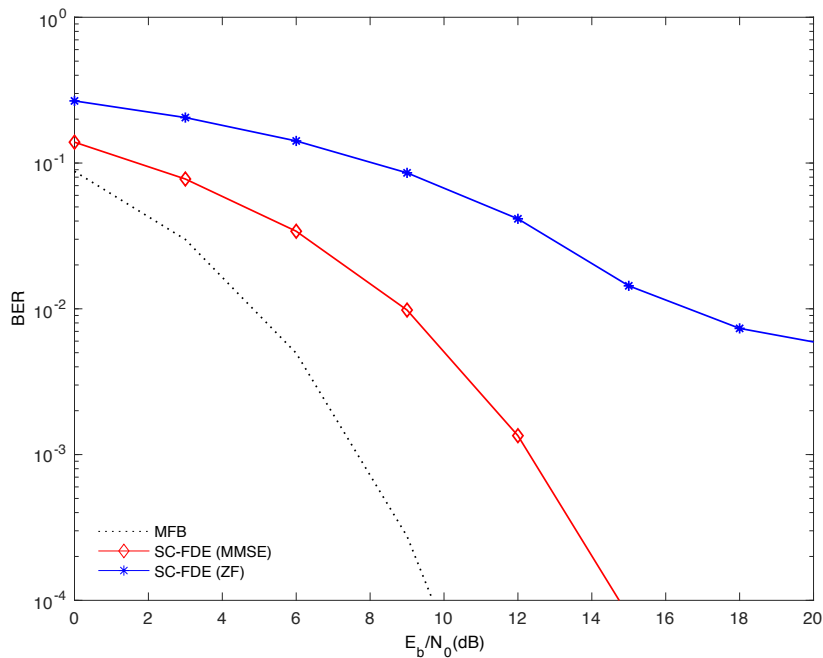


FIGURE 2.3: BER performance comparison for SC-FDE with ZF and MMSE equalization.

## 2.2.4 IB-FDE

The linear FDE used in both OFDM and SC-FDE schemes allows to achieve good performance. However, to increase the performance of SC-FDE, the linear FDE can be replaced by an IB-DFE, as initially proposed in [15]. This receiver includes two filters: the first one, the feedforward filter, equalizes most of the interference and the second one, the feedback filter, removes some of the residual interference. This is an iterative process that gradually increases the reliability of the received data. Still, this process may not be able to cancel the interference if the first detection is very bad [4]. The structure of this receiver is shown in Fig. 2.4.

In the  $i^{th}$  iteration, after the equalizer, the samples in the frequency-domain are  $\{\tilde{S}_k^{(i)}; k = 0, 1, \dots, N - 1\}$ , with

$$\tilde{S}_k^{(i)} = F_k^{(i)} Y_k - B_k^{(i)} \hat{S}_k^{(i-1)}, \quad (2.11)$$

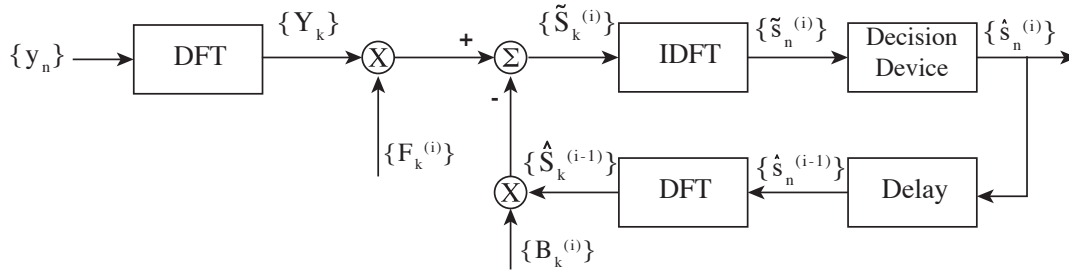


FIGURE 2.4: IB-DFE receiver structure.

where  $\{F_k^{(i)}; k = 0, 1, \dots, N - 1\}$  is the feedforward coefficient and  $\{B_k^{(i)}; k = 0, 1, \dots, N - 1\}$  is the feedback coefficient from the Decision-Feedback Equalizer (DFE) block. The "hard decision" sample from previous iteration is denoted as  $\{\hat{S}_k^{(i-1)}; k = 0, 1, \dots, N - 1\}$  and represents the DFT of the blocks  $\{\hat{s}_n^{(i-1)}; n = 0, 1, \dots, N - 1\}$  [16].

In order to maximize the Signal to Interference-plus-Noise Ratio (SINR) the feedforward coefficient must be

$$F_k^{(i)} = \frac{H_k^*}{\frac{1}{SNR} + (1 - (\rho^{(i-1)})^2)|H_k|^2} \quad (2.12)$$

and the feedback coefficients

$$B_k^{(i)} = \rho^{(i-1)}(F_k^{(i)} H_k - 1), \quad (2.13)$$

where  $\rho$  represents the correlation coefficient and is defined by

$$\rho^{(i)} = \frac{\mathbb{E}[\hat{S}_k^{(i)} S_k^*]}{\mathbb{E}[|S_k|^2]}. \quad (2.14)$$

The coefficient of correlation is a parameter that guarantees a good receiver performance because, in the feedback loop, the hard decisions for each block are taken into account, plus the overall reliability of the block, therefore reducing the propagation of errors.

In this type of iterative receiver and for the first iteration, i.e.,  $i = 1$ ,  $\rho = 0$

implies  $B_k^{(1)} = 0$  and  $F_k^{(1)}$  corresponding to equation 2.10. This happens since there is no information about  $s_n$  at this time. After this first iteration the coefficient  $B_k$  reduces a large part of residual ISI.

Fig. 2.5 shows the MFB and the BER performance of 4 iterations for the IB-DFE. As it is possible to verify, in the first iteration, for a value of  $\frac{Eb}{No} = 14.7$  dB we have a BER =  $10^{-4}$ . For this value of BER over the following iterations the value of  $\frac{Eb}{No}$  decreases to around 10.5 dB. It is also possible to see that the performance of iterations 3 and 4 is very similar and both approach the MFB, that is, the simulated samples approach the transmitted samples.

When a pulse is transmitted in an environment without ISI, it is possible to represent the best possible error performance for a receiver, that is, the MFB [17].

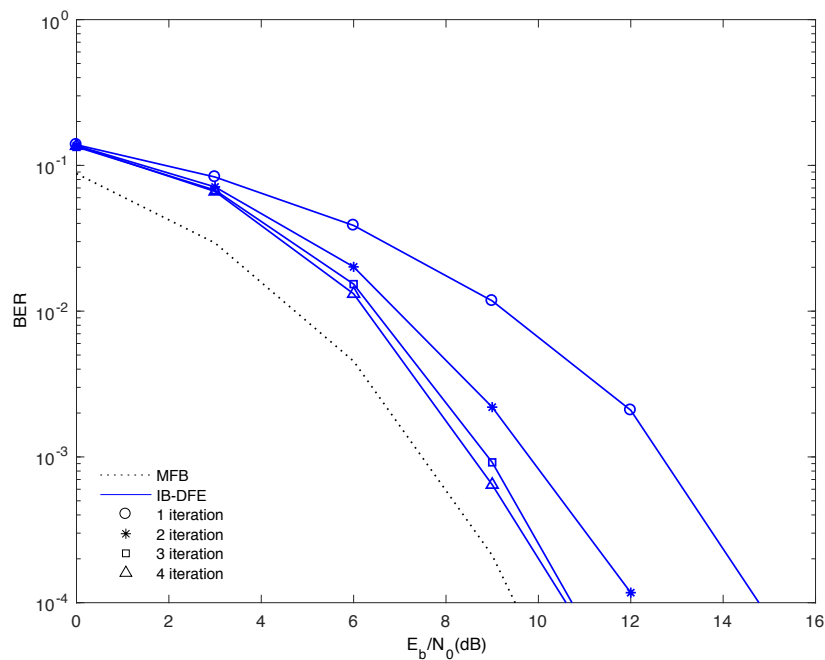


FIGURE 2.5: BER performance for an IB-DFE receiver with four iterations.

## 2.3 Multiple-Input, Multiple-Output systems

In this section the MIMO is initially presented, followed by the massive MIMO.

### 2.3.1 MIMO

In 1996, Foschini [18] demonstrated that multiple streams of data can be transmitted at the same frequency by establishing multiple parallel transmission channels. This is only possible if there are several antennas at both the transmitter and the receiver ends. The MIMO systems allow an increase on the reliability of transmission and the coverage area, thus increasing the throughput [19].

This type of MIMO systems undergoes frequency selective fading effects which decrease the performance achieved by the system. In order to minimize this effect, MIMO systems are combined with the OFDM technique. Thus MIMO-OFDM systems transform frequency selective fading into parallel flat fading, where all input signal frequencies suffer the same fading [20, 21, 22].

In order to increase the performance of MIMO-OFDM systems, the Singular Value Decomposition (SVD) linear processing technique can be used. This technique allows the MIMO channel to be decomposed into Single-Input, Single-Output (SISO) channels and can only be used if the channel matrix ( $\mathbf{H}_k$ ) is known to the transmitter and the receiver [21].

The SVD of  $\mathbf{H}_k$  it is given by:

$$\mathbf{H}_k = \mathbf{U}_k \mathbf{\Sigma}_k \mathbf{V}_k^H, \quad (2.15)$$

where  $\mathbf{U}_k$  and  $\mathbf{V}_k$  are unitary matrices with the columns representing the left and right singular vector of  $\mathbf{H}_k$ , respectively.  $\mathbf{\Sigma}_k$  is a matrix that in its diagonal contains the singular values of  $\mathbf{H}_k$ .

If at the transmitter  $s_n$  is processed by linear transformation  $s_n = \mathbf{V}s_n$  then the received signal is:

$$\mathbf{Y}_k = \mathbf{H}_k \mathbf{V}_k \mathbf{S}_k + \mathbf{N}_k. \quad (2.16)$$

By multiplying both elements by  $\mathbf{U}_k^H$  gives:

$$\mathbf{U}_k^H \mathbf{Y}_k = \mathbf{U}_k^H \mathbf{H}_k \mathbf{V}_k \mathbf{S}_k + \mathbf{U}_k^H \mathbf{N}_k. \quad (2.17)$$

Applying expression 2.15 results in

$$\mathbf{U}_k^H \mathbf{Y}_k = \mathbf{U}_k^H \mathbf{U}_k \boldsymbol{\Sigma}_k \mathbf{V}_k^H \mathbf{V}_k \mathbf{S}_k + \mathbf{U}_k^H \mathbf{N}_k. \quad (2.18)$$

As  $\mathbf{U}_k^H \mathbf{U}_k = \mathbf{I}$  and  $\mathbf{V}_k^H \mathbf{V}_k = \mathbf{I}$ , where  $\mathbf{I}$  represents the identity matrix, equation 2.18 simplifies to

$$\mathbf{U}_k^H \mathbf{Y}_k = \boldsymbol{\Sigma}_k \mathbf{S}_k + \mathbf{U}_k^H \mathbf{N}_k. \quad (2.19)$$

Therefore we conclude that it is possible to treat this system as having SISO channels.

However the main disadvantage of this technique is that the diversity of the signal allowed by the channel is not exploited [13, 21, 23, 24].

### 2.3.2 Massive MIMO

In order to comply with 5G specifications, there is a need to increase the data rate and to reduce the latency, therefore in [2, 3] the evolution of MIMO, known as massive MIMO, is studied. Massive MIMO systems work with dozens or hundreds of cheap and simple antennas [25]. With this increase of antennas it is possible to direct the energy in a single region, thus increasing the throughput and reducing the power loss.

Since the components are low-power and energy-efficient, it is possible to have devices that consume even less energy.

The existence of flat fading in these systems requires an increase in the transmitter power to ensure reliable transmission. As explained in section 2.3.1, it is possible to assume that each channel is only affected by flat fading, using OFDM, which greatly simplifies the analysis. However, and due to the problems presented at the beginning of section 2.2.3, for massive MIMO systems it is preferable to use SC-FDE [13].



# Chapter 3

## Receivers for Massive MIMO

This chapter shows some receivers that can be used in MIMO systems and be extended to massive MIMO systems. The following approach begins with a theoretical explanation and ends with the presentation of results obtained experimentally. Section 3.1 aims to present the extension of SC-FDE with IB-DFE for MIMO systems. In other words, this section will be the extension of section 2.2.4. A linear receiver, which has no iterations, is explained in section 3.2, posteriorly. Subsequently, linear low complexity receivers, MRC and EGC, are presented in sections 3.3 and 3.4, respectively.

### 3.1 IB-DFE for MIMO systems

In the previous chapter the concept of IB-DFE was associated with a system with an antenna to receive ( $R=1$ ) and an antenna to emit ( $P=1$ ), i.e., a SISO system. When passing to a MIMO system [26], with  $P \geq R$ , which is shown in Fig. 3.1, the block diagram shown in Fig. 2.4 may be extended to a block diagram for detecting the  $p^{th}$  MT presented in Fig. 3.2. For the  $i^{th}$  iteration,  $\tilde{S}_{k,p}^{(i)}$  is given by:

$$\tilde{S}_{k,p}^{(i)} = \mathbf{F}_{k,p}^{(i)T} \mathbf{Y}_k - \mathbf{B}_{k,p}^{(i)T} \bar{\mathbf{S}}_{k,p}^{(i-1)}, \quad (3.1)$$

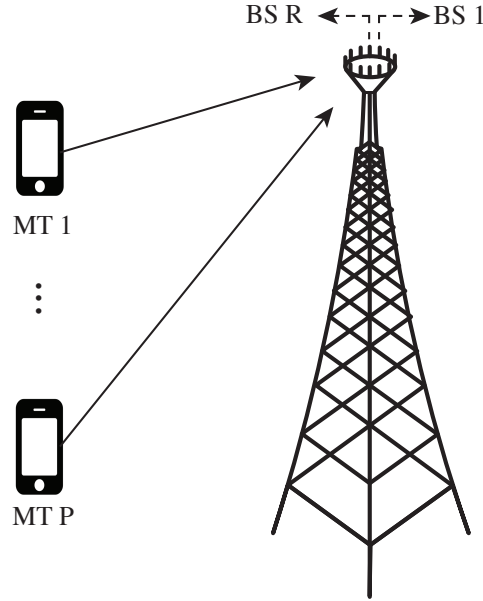


FIGURE 3.1: MIMO system.

where  $\mathbf{F}_{k,p}^{(i)T} = [F_{k,p}^{(i,1)}, \dots, F_{k,p}^{(i,R)}]$  and  $\mathbf{B}_{k,p}^{(i)T} = [B_{k,p}^{(i,1)}, \dots, B_{k,p}^{(i,P)}]$  with  $F_{k,p}$  and  $B_{k,p}$  represent feedforward and feedback coefficients, respectively [27].

Matrix  $\mathbf{Y}_k$  is given by:

$$\mathbf{Y}_k = [Y_k^{(1)}, \dots, Y_k^{(R)}]^T = \mathbf{H}_k \mathbf{S}_k + \mathbf{N}_k. \quad (3.2)$$

This equation (3.2) is analogous to equation 2.8 but in this case it is an extension for a case with more emitting and receiving antennas.  $\mathbf{H}_k$  denotes the  $R \times P$  channel matrix for the  $k^{th}$  frequency, with  $(r, p)^{th}$  element  $\mathbf{H}_k^{(r,p)}$ , and  $\mathbf{N}_k = [N_k^{(1)}, \dots, N_k^{(R)}]^T$  denotes the channel noise.

The DFT of the block in the time-domain  $\{\bar{s}_{s,p}^{(i)}; n = 0, 1, \dots, N - 1\}$ , for the  $p^{th}$  user and for the  $i^{th}$  iteration, is the block  $\{\bar{S}_{k,p}^{(i)}; k = 0, 1, \dots, N - 1\}$  whose elements constitute the vector  $\bar{\mathbf{S}}_{k,p}^{(i-1)} = [\bar{S}_{k,1}^{(i)}, \bar{S}_{k,p-1}^{(i)}, \bar{S}_{k,p}^{(i-1)}, \dots, \bar{S}_{k,P}^{(i-1)}]^T$ . The elements  $\bar{s}_{n,p}$  and  $\bar{S}_{k,p}$  represent the "soft decisions" in the time domain and frequency domain, respectively. Once the "soft decisions" do "symbol averages" and the "hard decisions" do "blockwise average" [28] the following relationship

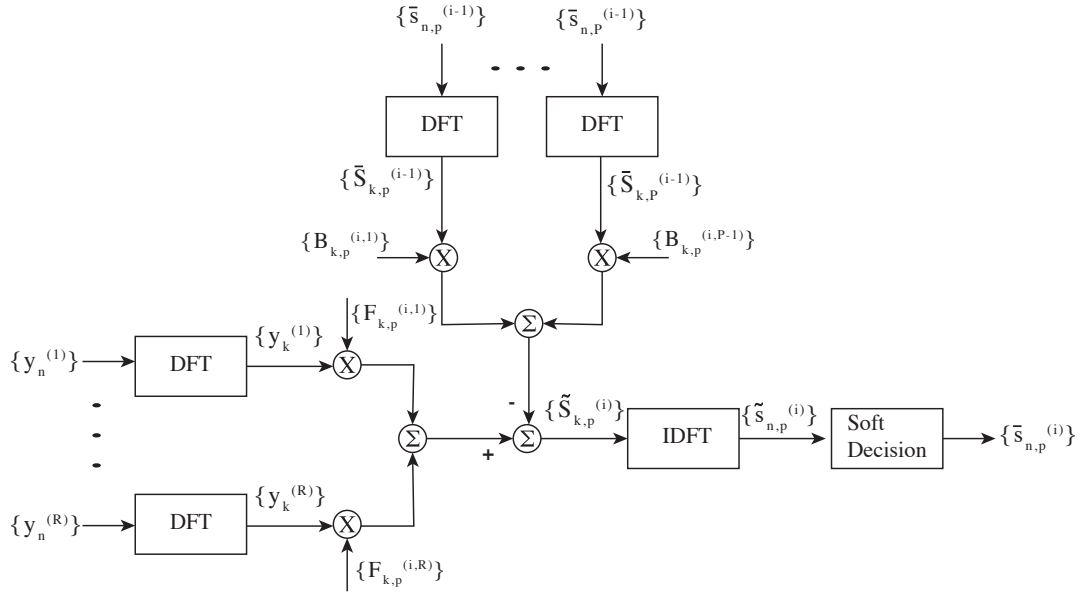


FIGURE 3.2: MIMO IB-DFE receiver structure.

can be written:

$$\bar{\mathbf{S}}_k^{(i-1)} \simeq \mathbf{P}^{(i-1)} \tilde{\mathbf{S}}_k^{(i)}, \quad (3.3)$$

where

$$\mathbf{P}^{(i-1)} = \text{diag}(\rho_1^{(i-1)}, \dots, \rho_P^{(i-1)}). \quad (3.4)$$

The correlation coefficient  $\rho_P^{(i-1)}$  defined in equation 2.14 and  $\tilde{\mathbf{S}}_k^{(i)}$  can be approximated by:

$$\tilde{\mathbf{S}}_k^{(i)} \approx \mathbf{P}^{(i-1)} \mathbf{S}_k + \mathbf{\Delta}_k. \quad (3.5)$$

In equation 3.5 the coefficient  $\mathbf{\Delta}_k = [\Delta_{k,1}, \dots, \Delta_{k,P}]^T$  has zero mean and it is uncorrelated with  $\mathbf{P}^{(i-1)}$ . When the first iteration is considered,  $i = 1$ ,  $\mathbf{P}^{(0)}$  is a null matrix which implies that  $\tilde{\mathbf{S}}_k^{(0)}$  is a null vector [29].

The BER performance of the IB-DFE receiver for a MIMO case, i.e., 2 MTs transmit to 6 BSs ( $R/P = 3$ ), is shown in Fig. 3.3. As it is possible to verify, the iterations 2, 3 and 4 present very similar performance among themselves and are very close to the MFB, at about 0.4 dB. The first iteration of this receiver to a

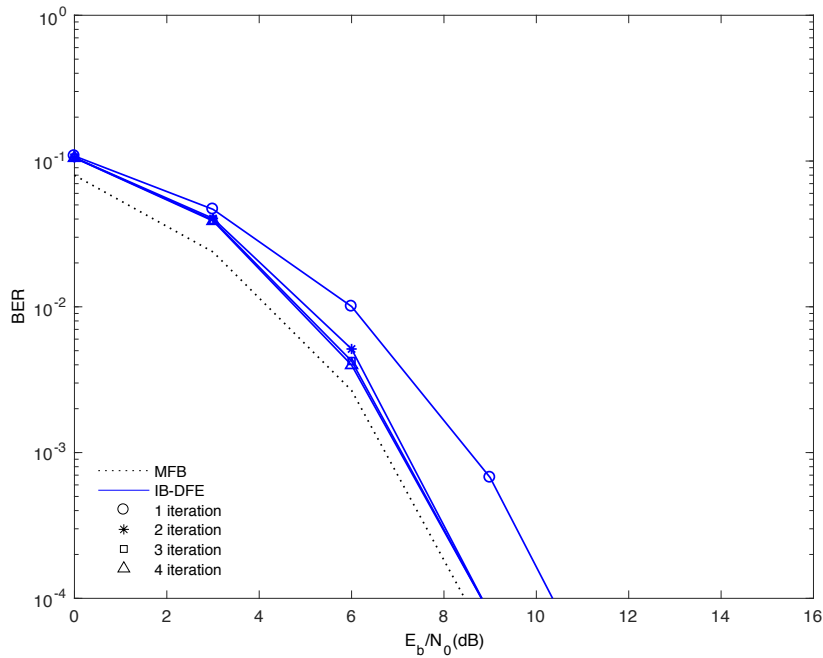


FIGURE 3.3: BER performance for IB-DFE receiver with  $P = 2$  MTs and  $R = 6$  BSs.

BER =  $10^{-4}$  has an  $\frac{Eb}{No}$  of approximately 10.3 dB, which is 1 dB higher than the remaining iterations.

When the use of this receiver is extended to a system with 60 MTs and 180 BSs ( $R/P = 3$ ), i.e. a massive MIMO system, the performance obtained is shown in Fig.3.4. It is possible to verify that the 4 iterations present the same progress until they reach an  $\frac{Eb}{No} = 6$  dB corresponding to a BER  $\approx 10^{-2}$ . The BER =  $10^{-4}$  is reached in the first iteration when the  $\frac{Eb}{No} = 10$  dB and in the fourth iteration when  $\frac{Eb}{No} \approx 8.5$  dB.

As the  $R/P$  increases to 6, as represented in Fig. 3.5, the performance achieved by the receiver is identical to the previous case (Fig. 3.4), so the second, third and fourth iterations are coincident with each other and reach a BER =  $10^{-4}$  for  $\frac{Eb}{No} \approx 8.4$  dB. It can then be verified that the receiver under study presents a similar performance on both the MIMO system and the massive MIMO system. As we can verify, an increase of  $R/P$  does not significantly affect the performance of the receiver in massive MIMO systems.

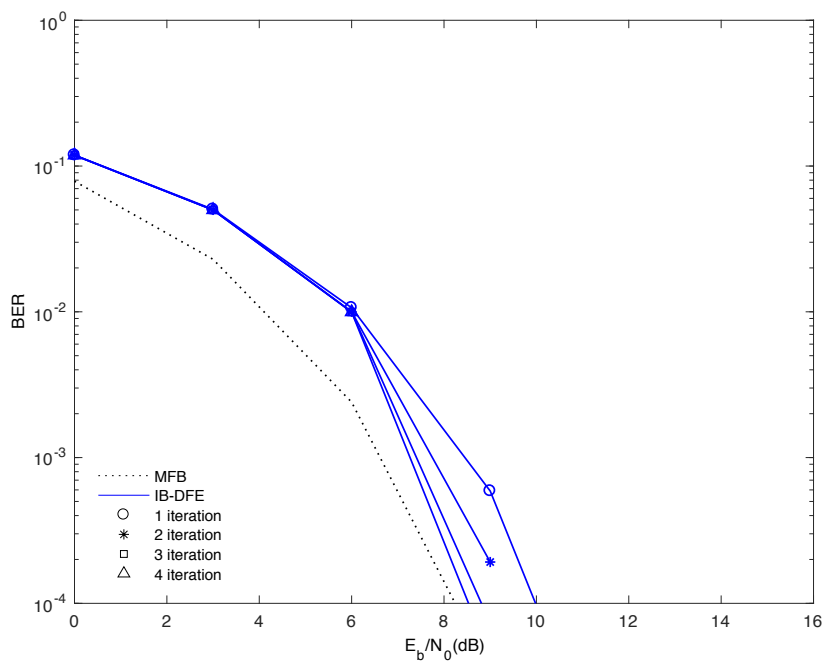


FIGURE 3.4: BER performance for IB-DFE receiver with  $P = 60$  MTs and  $R = 180$  BSs.

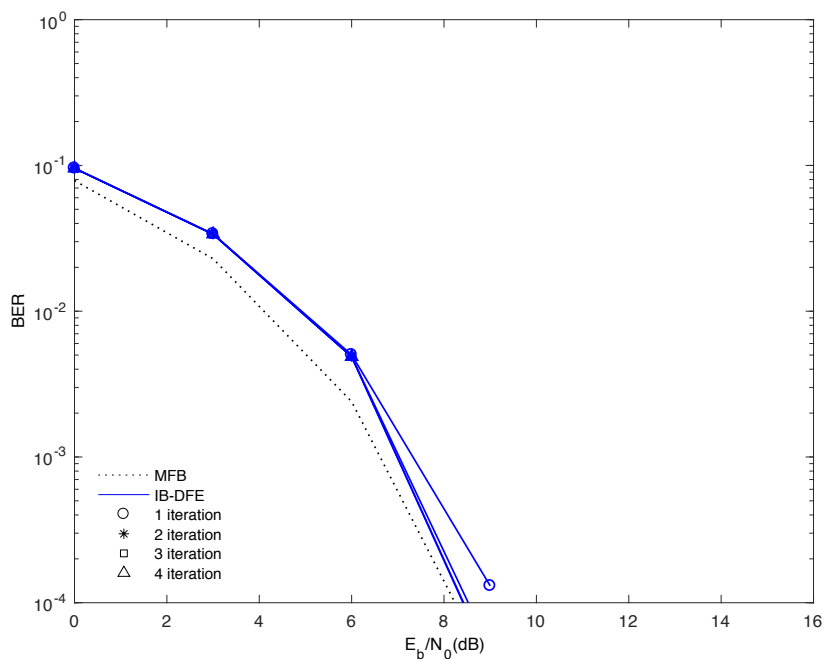


FIGURE 3.5: BER performance for IB-DFE receiver with  $P = 60$  MTs and  $R = 360$  BSs.

Despite the excellent performance achieved by this receiver for massive MIMO systems, the algorithm followed presents many matrix manipulations, as previously stated.

Since the complexity of matrix operations depends on their size and once these matrices have very large dimensions, the complexity of the operations makes these receivers not suitable for massive MIMO systems.

## 3.2 Zero Forcing

In the previous section, an iterative receiver was analyzed that approached the MFB after some iterations. However this type of receiver presents some problems due to its computational complexity. In this section a linear receiver, the Zero Forcing (ZF), is presented.

In this receiver, after the equalizer, the frequency-domain samples  $\tilde{\mathbf{S}}_k$  are given by:

$$\tilde{\mathbf{S}}_k = \left[ \tilde{S}_k^{(1)}, \dots, \tilde{S}_k^{(R)} \right]^T = \mathbf{F}_k^T \mathbf{Y}_k = (\mathbf{H}_k \mathbf{H}_k^H + \alpha \mathbf{I})^{-1} \mathbf{H}_k^H \mathbf{Y}_k, \quad (3.6)$$

where  $\mathbf{I}$  represents the identity matrix and  $\alpha = \frac{\mathbb{E}[|N_k^{(r)}|^2]}{\mathbb{E}[|S_k^{(p)}|^2]}$  is assumed identical for all values of  $r$  and  $p$  [30]. For the receiver under study  $\alpha = 0$  which simplifies the previous equation to:

$$\tilde{\mathbf{S}}_k = (\mathbf{H}_k \mathbf{H}_k^H)^{-1} \mathbf{H}_k^H \mathbf{Y}_k. \quad (3.7)$$

Similarly to the receiver presented in the previous section, this one also presents the necessity of channel inversion for each one of the  $k$  frequencies, which makes it too heavy computationally when used for massive MIMO systems.

Fig. 3.6 shows the BER performance of the ZF receiver in the case of a MIMO system. Figures 3.7 and 3.8 show the BER performance of the ZF receiver in a massive MIMO system. In these figures, the BER performance for the IB-DFE receiver is also presented because in both systems the BER performance of the ZF coincides, almost totally, with the 1<sup>st</sup> iteration of the IB-DFE. Another conclusion

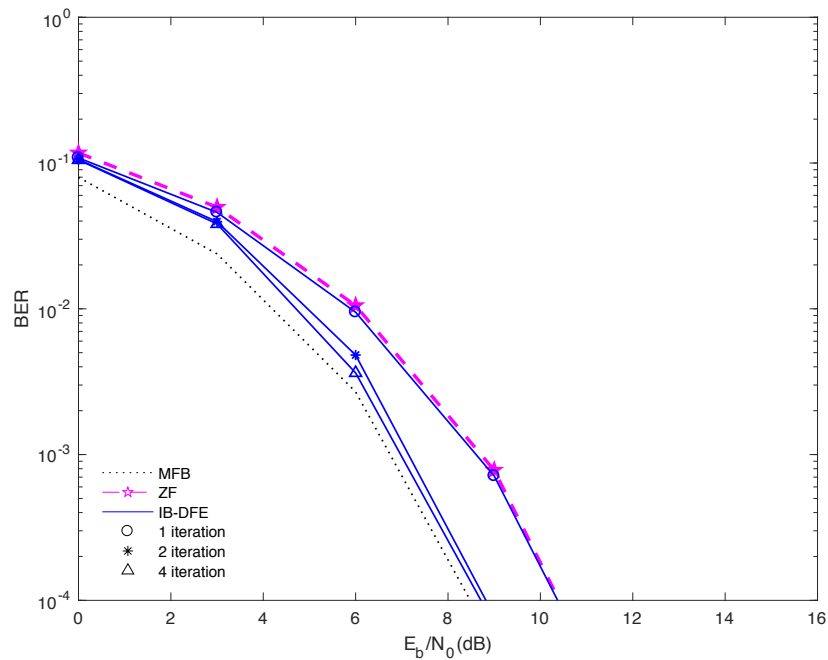


FIGURE 3.6: BER performance for IB-DFE and ZF receivers with  $P = 2$  MTs and  $R = 6$  BSs.

that can be drawn is that for massive MIMO systems the increase of  $R/P$  does not modify the performance achieved by this receiver.

As this receiver is not an iterative receiver and its performance is very similar to the first iteration of the IB-DFE, which only differs 1.9 dB from the MFB at  $\text{BER} = 10^{-4}$ , this receiver will not be considered in section 4.3, which compares different receivers.

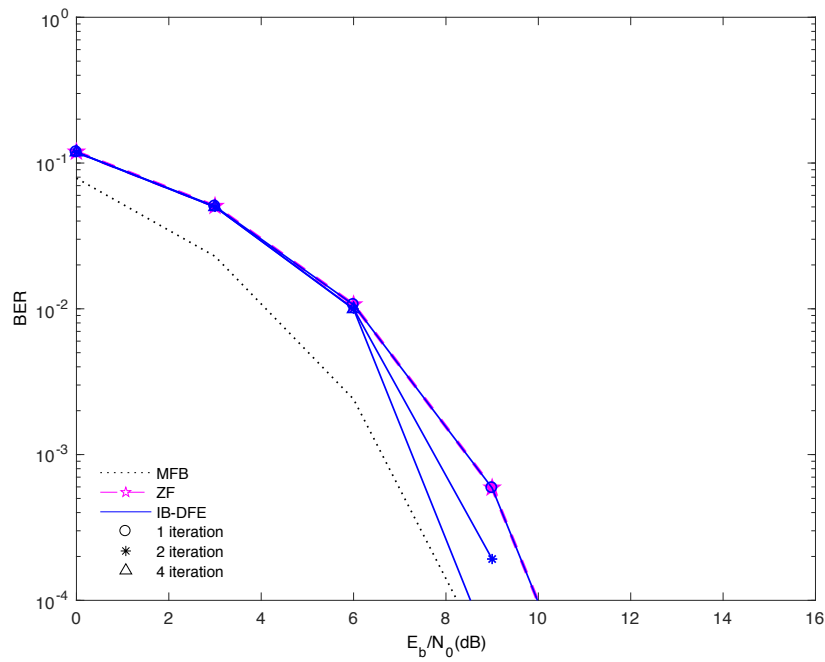


FIGURE 3.7: BER performance for IB-DFE and ZF receivers with  $P = 60$  MTs and  $R = 180$  BSs.

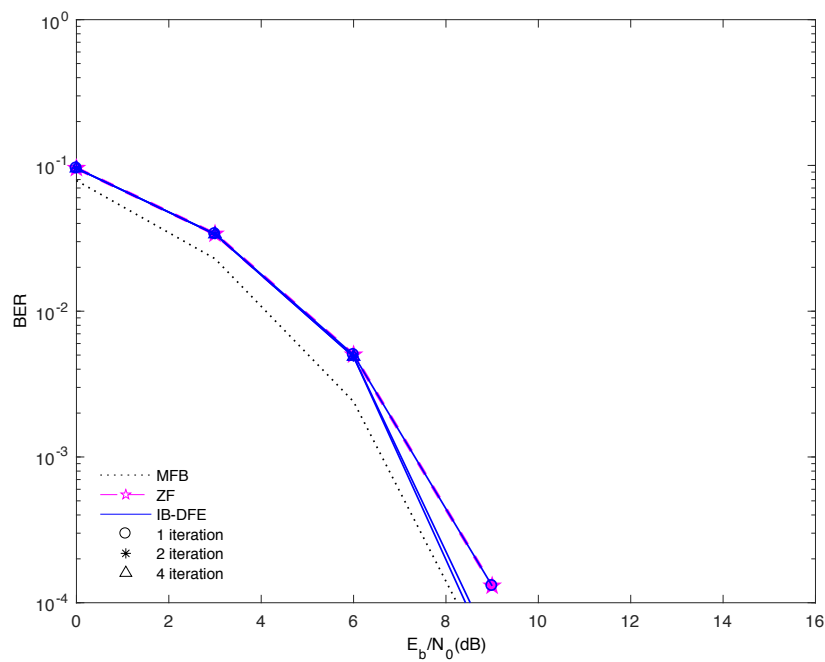


FIGURE 3.8: BER performance for IB-DFE and ZF receivers with  $P = 60$  MTs and  $R = 360$  BSs.



### 3.3 Linear MRC

As seen in the previous section, IB-DFE receivers present an excellent performance, however, its algorithm includes too many matrix inversions which increases their computational load. For massive MIMO systems, it is fundamental to think of an algorithm that is simpler and does not involve the inversion of matrices such as the Maximal-Ratio Combining (MRC).

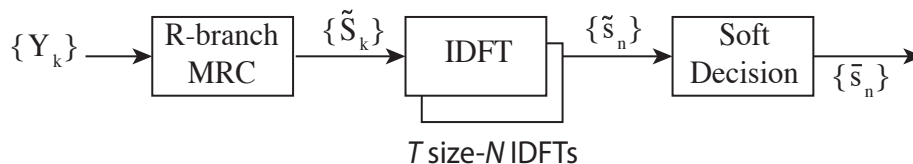


FIGURE 3.9: Massive MIMO receiver and equalization for linear MRC.

At the MRC receiver, the signal from each branch is multiplied by a weight factor proportional to the signal amplitude of that branch. So, if a branch presents a weak signal it will be attenuated while a branch with a strong signal will be amplified [31, 32].

The problem of the ZF receiver is related to the channel inversion so, in the case of the MRC, the approximation presented in expression 3.8 simplifies the receiver.

$$\mathbf{H}_k \mathbf{H}_k^H \approx R \mathbf{I}, \quad (3.8)$$

with  $\mathbf{I}$  corresponding to the identity matrix. When  $R \gg 1$  the correlation between the channels among different transmit and receive antennas is very small [30]. Thus expression 3.7 of the ZF receiver can be simplified to

$$\tilde{\mathbf{S}}_k^{(i)} = \Psi \mathbf{H}_k^H \mathbf{Y}_k, \quad (3.9)$$

where the diagonal of the matrix is represented by  $\Psi$  and the element  $(p, p)^{th}$  is given by:

$$\left( \sum_{k=0}^{N-1} \sum_{r=1}^R |\mathbf{H}_k^{(r,p)}|^2 \right)^{-1}. \quad (3.10)$$

The block diagram of this receiver is shown in Fig. 3.9. Expression 3.10 ensures that the overall frequency response of the "channel plus receiver" for each MT has average 1.

The performance of this linear receiver is represented in figures 3.10, 3.11 and 3.12 together with the receiver performance studied in the next section.

### 3.4 Linear EGC

In this section we present another low complexity receiver: the Equal Gain Combining (EGC).

This receiver does not require channel estimation which makes its implementation simpler when compared to the MRC. In the case of EGC, regardless of signal amplitude of each branch, all branches are weighted by the same factor. In order to avoid the cancellation of the signal, it is necessary to co-phase all the signals [31].

Like in the MRC receiver, when  $R \gg 1$ , the small correlation between the signals from the different emitters and receivers is very small [33]. Thus, the elements outside the diagonal of expression 3.11 are much lower than those of the diagonal.

$$\mathbf{A}_k^H \mathbf{H}_k. \quad (3.11)$$

The elements of the diagonal of  $\mathbf{A}$ , i.e., the  $(i, i')^{th}$  elements are given by:

$$[\mathbf{A}]_{i,i'} = \exp\left(j \arg\left([\mathbf{H}]_{i,i'}\right)\right), \quad (3.12)$$

so the phase corresponds to the element of matrix  $\mathbf{H}$  and the absolute value is 1.

The receiver and equalization scheme of this receiver is similar to that shown in Fig. 3.9, its only difference being the block corresponding to the "R-branch MRC" which should be replaced by a "R-branch EGC".

At this receiver, the matrix  $\tilde{\mathbf{S}}_k^{(i)}$  is given by:

$$\tilde{\mathbf{S}}_k^{(i)} = \Psi \mathbf{H}_k^H \mathbf{Y}_k, \quad (3.13)$$

Fig. 3.10 shows the performance of linear MRC and EGC receivers in a MIMO system and in figures 3.11 and 3.12 a massive MIMO system is considered. In these figures the number of receiving antennas ( $R$ ) was varied in order to obtain different  $R/P$  values.

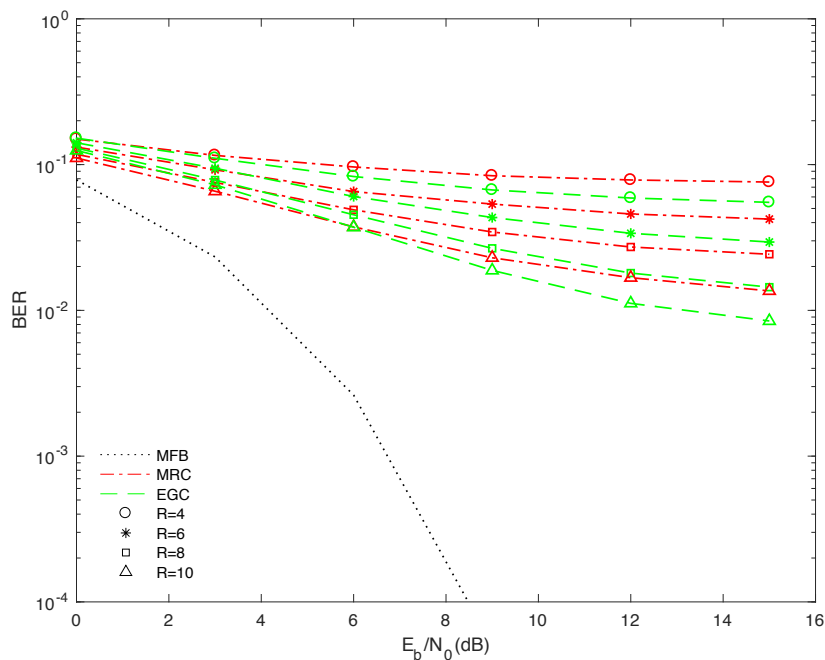


FIGURE 3.10: BER performance for MRC and EGC receivers with  $P = 2$  MTs and different values of  $R$  BSs.

In the case of the MIMO system (Fig. 3.10), the EGC receiver performs better in comparison to the MRC receiver, however the performance achieved by these receivers is very poor, since the values of BER are too high. It is also possible to verify that with the increase of  $R/P$  the performance improves slightly, but even so the best performance that these receivers present for an  $\frac{E_b}{N_0} = 15$  dB is BER =  $8 \times 10^{-3}$  for the case of EGC and a BER  $\approx 10^{-2}$ , for the case of the MRC with a  $R/P = 5$ .

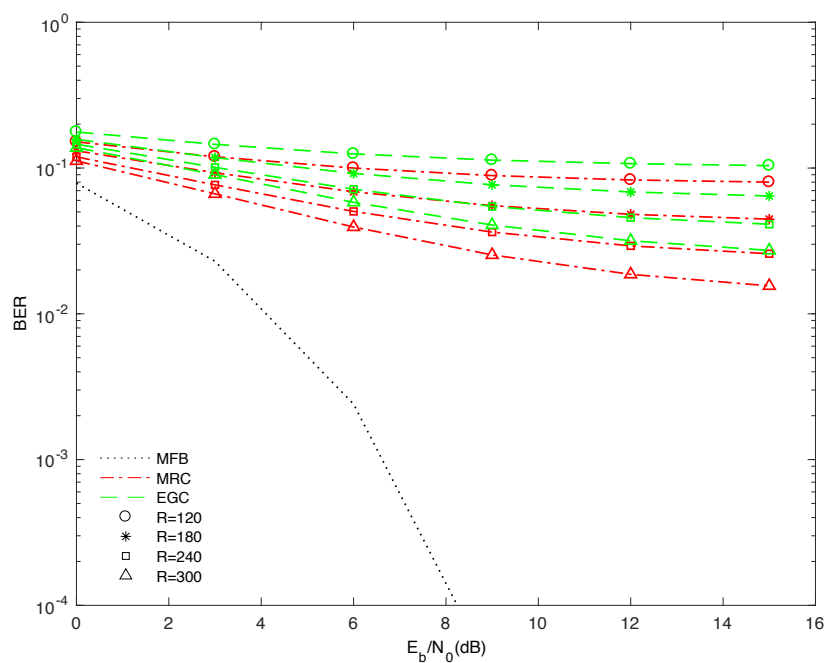


FIGURE 3.11: BER performance for MRC and EGC receivers with  $P = 60$  MTs and different values of  $R$  BSs.

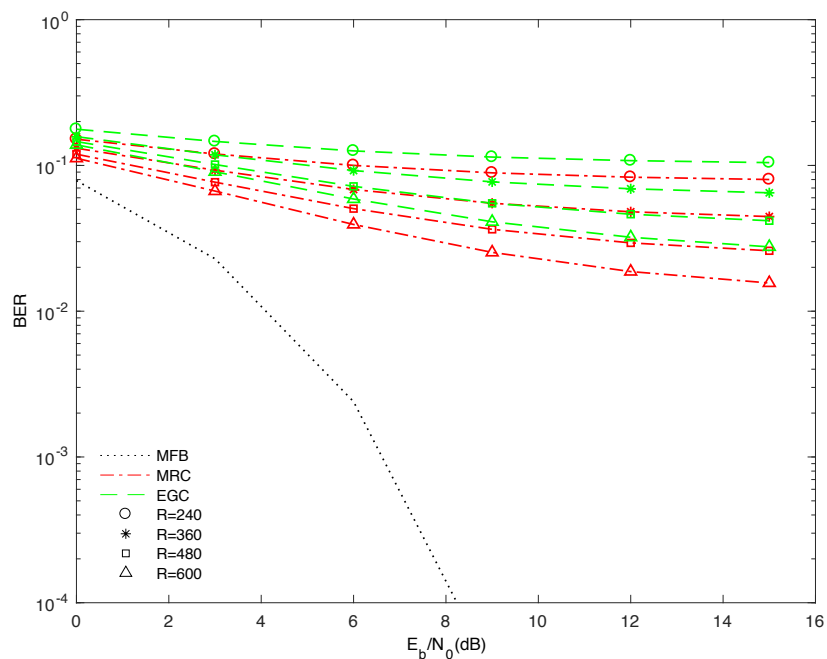


FIGURE 3.12: BER performance for MRC and EGC receivers with  $P = 120$  MTs and different values of  $R$  BSs.

Considering the massive MIMO system (figures 3.11 and 3.12) the performance achieved with the receivers is similar to the MIMO system. In this type of systems, the MRC receiver achieves better performance than the EGC receiver, and when  $R/P = 5$ , for an  $\frac{E_b}{N_o} = 15$  dB, a BER =  $1.5 \times 10^{-2}$  is reached. It is possible to verify that when doubling the number of emitting antennas, and maintaining the same  $R/P$  relationship, the performance reached by these receivers is very similar.



# Chapter 4

## Low complexity receivers for Massive MIMO systems

The receivers shown in chapter 3 presented some problems such as their implementation complexity or their poor performance. In this chapter low complexity iterative receivers that can be used in MIMO systems are presented.

This chapter begins with the presentation iterative versions for the MRC and EGC receivers, in sections 4.1 and 4.2 respectively. In section 4.3 a comparison between the different iterative receivers studied is presented. Finally, in section 4.4 a receiver that tries to overcome the previous drawbacks is proposed.

### 4.1 Iterative MRC

As shown in the previous chapter, the linear receiver MRC presented a very poor performance and with the increase of  $R/P$  it has to take into account the residual interference. Thus, the linear receiver presented previously used iterations to reduce this interference. The iterative MRC receiver is shown in Fig. 4.1 [30] and the corresponding  $\tilde{\mathbf{S}}_k^{(i)}$  is given by:

$$\tilde{\mathbf{S}}_k^{(i)} = \Psi \mathbf{H}_k^H \mathbf{Y}_k - \mathbf{B}_k^{(i)} \bar{\mathbf{S}}_k^{(i-1)}, \quad (4.1)$$

where  $\mathbf{B}_k^{(i)}$  reduces interference between users and ISI and is given by:

$$\mathbf{B}_k^{(i)} = \Psi \mathbf{H}_k^H \mathbf{H}_k - \mathbf{I}. \quad (4.2)$$

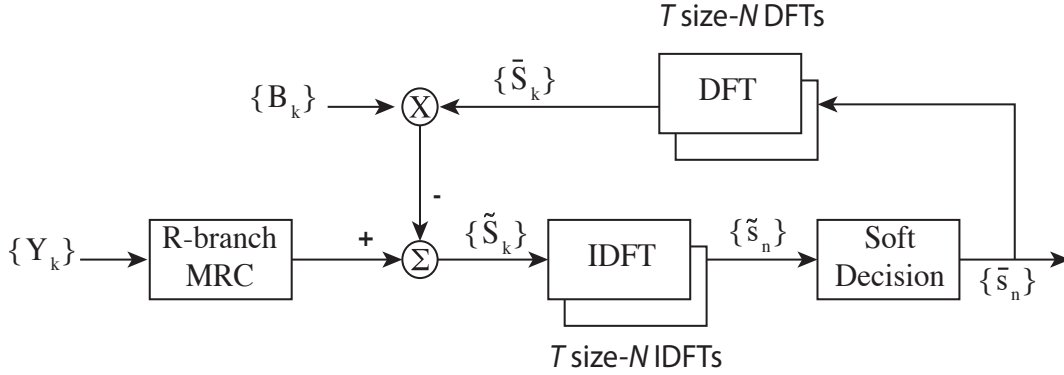


FIGURE 4.1: Massive MIMO receiver and equalization for iterative MRC.

Still, in expression 4.1 we have the element  $\bar{\mathbf{S}}_k^{(i)} = [\bar{S}_0^{(i)}, \dots, \bar{S}_{N-1}^{(i)}]$  that represents the average values, in the frequency domain, conditioned to the FDE output of the previous iteration. This output can be computed as explained in section 3.1. In the first iteration, i.e.  $i = 1$ , there is no previous information  $\bar{\mathbf{S}}_k^{(0)} = 0$ , which causes the receiver to be viewed as a linear MRC. In the following iterations, the results from previous iterations are used to reduce ISI and interference between users.

With the increase on the number of iterations, for moderate-to-high SNR values, the average of the receiver's output is close to the transmitted signals, which indicates that the interference cancellation performed by the  $\mathbf{B}_k$  element becomes more efficient, leading to an increase in the receiver performance.

In Fig. 4.2 the BER performance of an MRC receiver with 4 iterations for a MIMO system is presented. In the first iteration this receiver has a low slope curve which for  $\frac{Eb}{No} = 15$  dB has  $\text{BER} \approx 4 \times 10^{-2}$ . For the second iteration, with  $\frac{Eb}{No} = 15$  dB achieves a performance of  $10^{-3}$ . For iterations 3 and 4 up to  $\frac{Eb}{No} = 9$



dB the curves present the same progress towards the MFB. For higher  $\frac{E_b}{N_0}$  values the curves depart from the MFB. In short, this receiver is only efficient for more than 4 iterations. It can also be emphasized that in none of these 4 iterations, the receiver reaches a BER of  $10^{-4}$ .

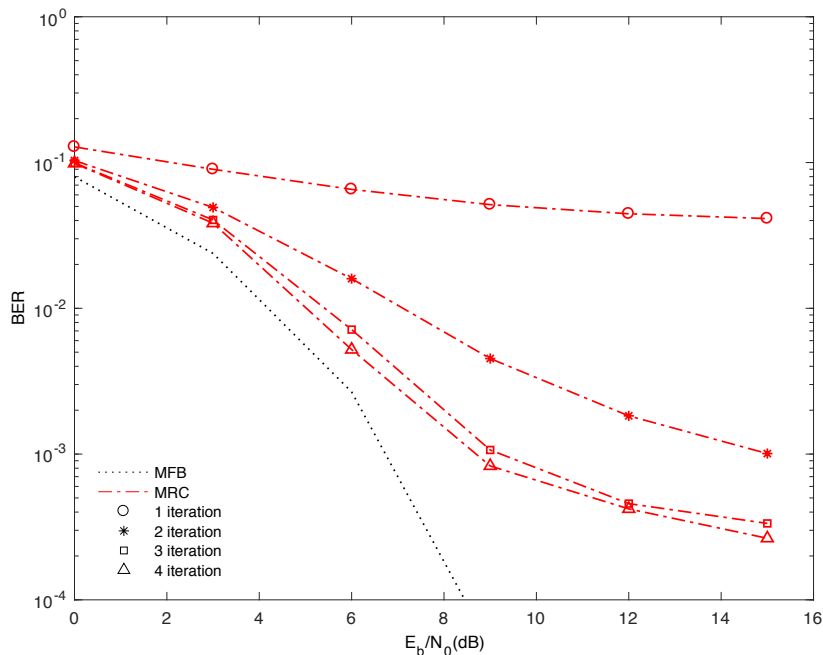


FIGURE 4.2: BER performance for MRC receiver with  $P = 2$  MTs and  $R = 6$  BSs.

When the system being studied is a massive MIMO, the performance of the MRC is much better, as shown in figures 4.3 and 4.4. In the case of  $R/P = 3$ , shown in Fig. 4.3, and for the first iteration, the performance of the receiver is quite poor. However the second iteration already reaches a BER =  $10^{-4}$  when  $\frac{E_b}{N_0} = 14.4$  dB, only 6.2 dB apart from the MFB. Iterations 3 and 4 present a very close performance to the MFB, and for a BER =  $10^{-4}$  the 3<sup>rd</sup> iteration already presents  $\frac{E_b}{N_0} = 8.6$  dB and for the 4<sup>th</sup> iteration  $\frac{E_b}{N_0} = 8.3$  dB that is only 0.03 dB away from the MFB.

When  $R/P = 6$ , as shown in Fig. 4.4, the performance improves reasonably in comparison with the  $R/P = 3$  case. The first iteration reaches a BER  $\approx 10^{-2}$  when  $\frac{E_b}{N_0} = 15$  dB and the second iteration for BER =  $10^{-4}$  is about 0.8 dB

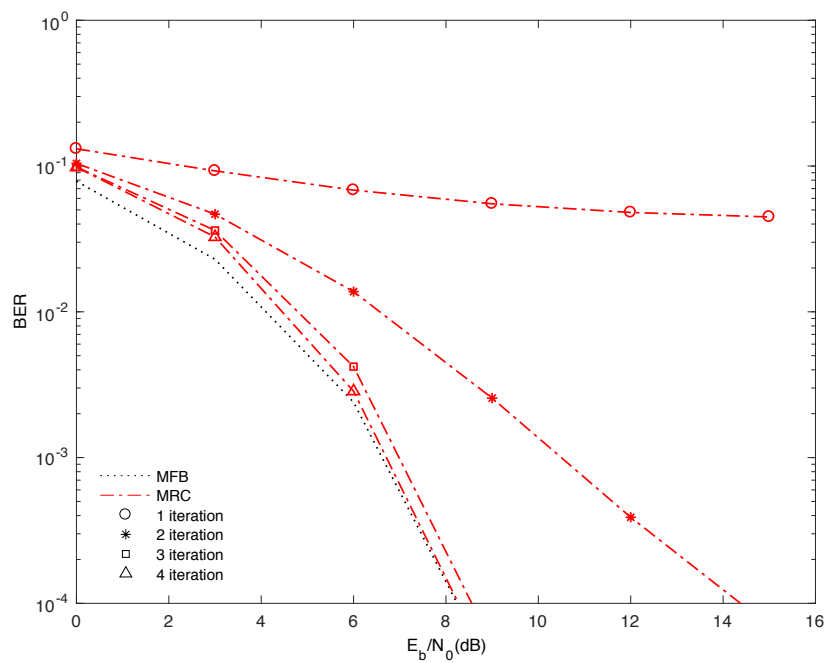


FIGURE 4.3: BER performance for MRC receiver with  $P = 60$  MTs and  $R = 180$  BSs.

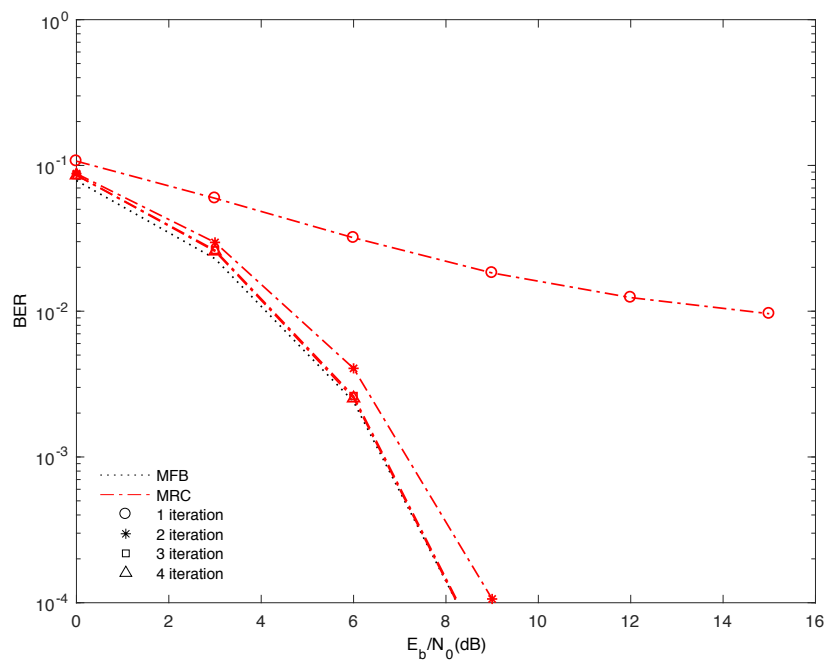


FIGURE 4.4: BER performance for MRC receiver with  $P = 60$  MTs and  $R = 360$  BSs.

from the MFB, which demonstrates the improvement on the performance with the increase of  $R/P$ . The performance achieved with iterations 3 and 4 coincides almost entirely with the performance of MFB.

Therefore, these results show that the performance achieved after only 3 iterations is quite good, especially when  $R/P$  is substantial, allowing its use in massive MIMO systems.

## 4.2 Iterative EGC

For MRC receiver, with high  $R/P$ , the interference between users and the ISI also increases, so it is important to define a factor that can minimize these effects. This factor,  $\mathbf{B}_k^{(i)}$ , is given by equation:

$$\mathbf{B}_k^{(i)} = \Psi \mathbf{A}_k^H \mathbf{H}_k - \mathbf{I}. \quad (4.3)$$

The calculation of  $\tilde{\mathbf{S}}_k^{(i)}$  is given by [33]:

$$\tilde{\mathbf{S}}_k^{(i)} = \Psi \mathbf{H}_k^H \mathbf{Y}_k - \mathbf{B}_k^{(i)} \tilde{\mathbf{S}}_k^{(i-1)}. \quad (4.4)$$

The same assumptions for the MRC receiver can also be taken for the EGC receiver, that is, for the 1<sup>st</sup> iteration the receiver can be seen as a linear EGC receiver and with the increase in the number of iterations its performance increases, since the cancellation done by matrix  $\mathbf{B}_k$  becomes more efficient.

The BER performance of the EGC receiver for MIMO systems and massive MIMO systems is shown in figures 4.5, 4.6 and 4.7. It can be verified that for both systems the first iteration is very poor not converging to the MFB. In this case, a performance similar to the MFB performance is also achieved.

For MIMO systems, shown in Fig. 4.5, the second iteration, a BER =  $10^{-4}$  is reached when  $\frac{E_b}{N_o} = 14$  dB. The performance for the 3<sup>rd</sup> and 4<sup>th</sup> iterations show

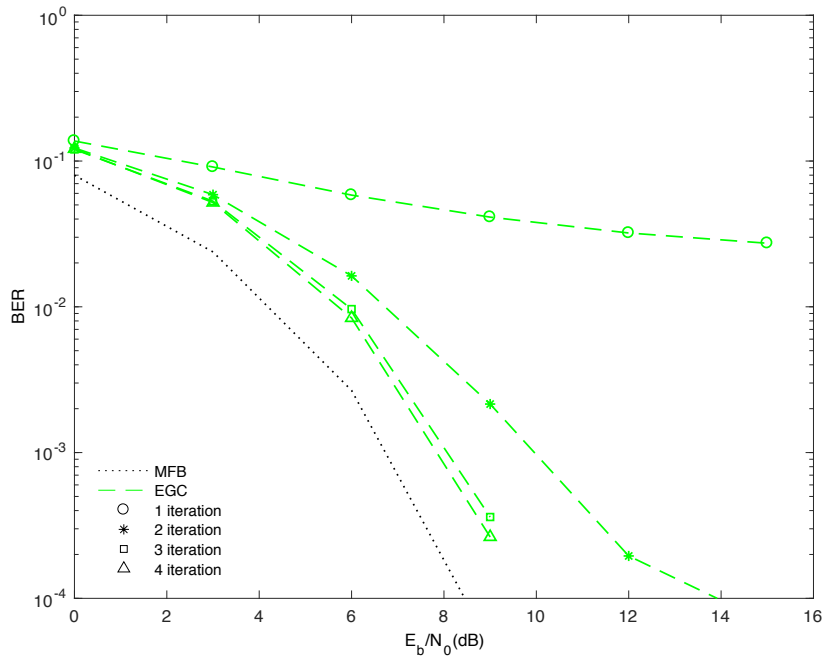


FIGURE 4.5: BER performance for EGC receiver with  $P = 2$  MTs and  $R = 6$  BSs.

the same progress as the performance of the MFB over the increase of  $\frac{E_b}{N_0}$ , however these curves for a similar value of BER are now separated by about 1.2 dB and 1 dB from the MFB, respectively.

In the case of massive MIMO systems, shown in figures 4.6 and 4.7, the first iteration curve is practically flat. In the case of  $R/P = 3$ , Fig. 4.6, the 2<sup>nd</sup> iteration never reaches a BER =  $10^{-4}$ . When  $\frac{E_b}{N_0} = 10$  dB the 3<sup>rd</sup> iteration presents a BER =  $10^{-4}$  and the performance for the 4<sup>th</sup> iteration reaches 1.2 dB from the MFB. With the increase of  $R/P$  to 6, Fig. 4.7, the receiver performance improves as the second iteration reaches a BER =  $10^{-4}$  for an  $\frac{E_b}{N_0} = 10.5$  dB. The 3<sup>rd</sup> and 4<sup>th</sup> iterations are coincident and are only separated 1 dB from the MFB.

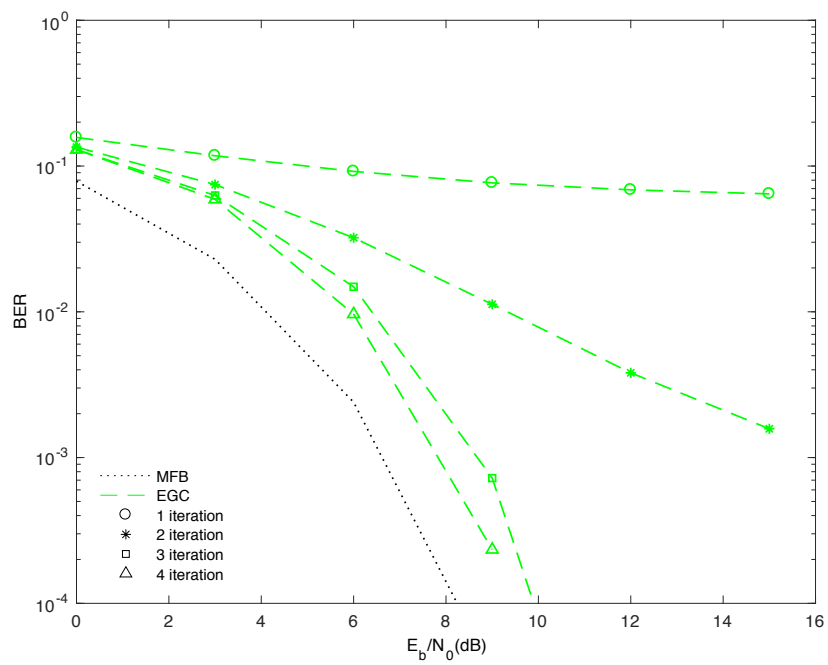


FIGURE 4.6: BER performance for EGC receiver with  $P = 60$  MTs and  $R = 180$  BSs.

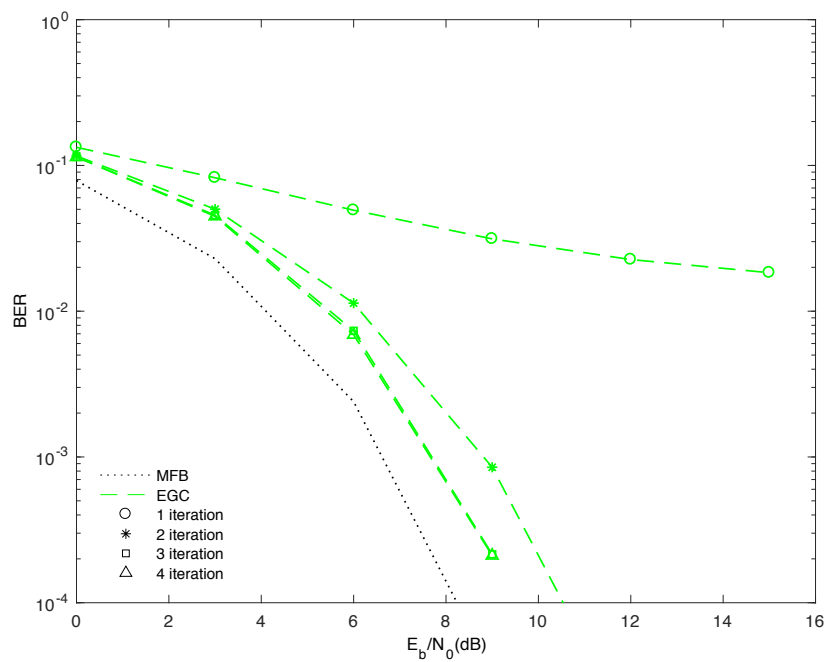


FIGURE 4.7: BER performance for EGC receiver with  $P = 60$  MTs and  $R = 360$  BSs.

### 4.3 Comparison between receivers

In this section it is possible to compare the BER performance for the IB-DFE, MRC and EGC receivers. Firstly it is considered a massive MIMO system with 60 MTs and 180 BSs, i.e.,  $R/P = 3$  and later on the system considers  $R/P = 6$ , being composed of 60 MTs and 360 BSs.

In figures 4.8 and 4.9 it is possible to compare the first 4 iterations of the IB-DFE receiver with the MRC receiver. When  $R/P = 3$ , Fig. 4.8, the 1<sup>st</sup> and 2<sup>nd</sup> iterations of the MRC give bad results, and its performance is worse than that of the first iteration with IB-DFE. However for a  $\text{BER} = 10^{-4}$  the curve for the fourth iteration of the IB-DFE is 0.5 dB away from the MFB while the 4<sup>th</sup> iteration of the MRC coincides with the MFB.

When  $R/P$  is increased to 6, Fig. 4.9, the performance of both receivers improves. Although the 1<sup>st</sup> iteration of the MRC does not provide good results, the 2<sup>nd</sup> iteration provides the performance of the 1<sup>st</sup> iteration of the IB-DFE. The performance resulting from the 4<sup>th</sup> iteration of the MRC coincides with that of the MFB, and is about 0.2 dB better, than that achieved by the IB-DFE.

It can be concluded that, for a receiver with only one iteration, the IB-DFE receiver is the only technique that achieves the best performance, although presenting too much complexity for this type of systems. When the four iterations are considered, the MRC exhibits an excellent performance, which nearly coincides with the MFB, and does not have the complexity of the IB-DFE.

When comparing IB-DFE with the low complexity EGC receiver, as shown in figures 4.10 and 4.11, it is again possible to verify that the first iteration of the low complexity receiver does not give good results, in fact much worse than those of the IB-DFE iterations.

In the case shown in Fig. 4.10, with  $R/P = 3$ , the results provided by the 4<sup>th</sup> iteration of the EGC are only 1 dB away of the MFB, for a  $\text{BER} = 10^{-4}$ , and coincide when the second iteration of the IB-DFE is applied. The 4<sup>th</sup> iteration

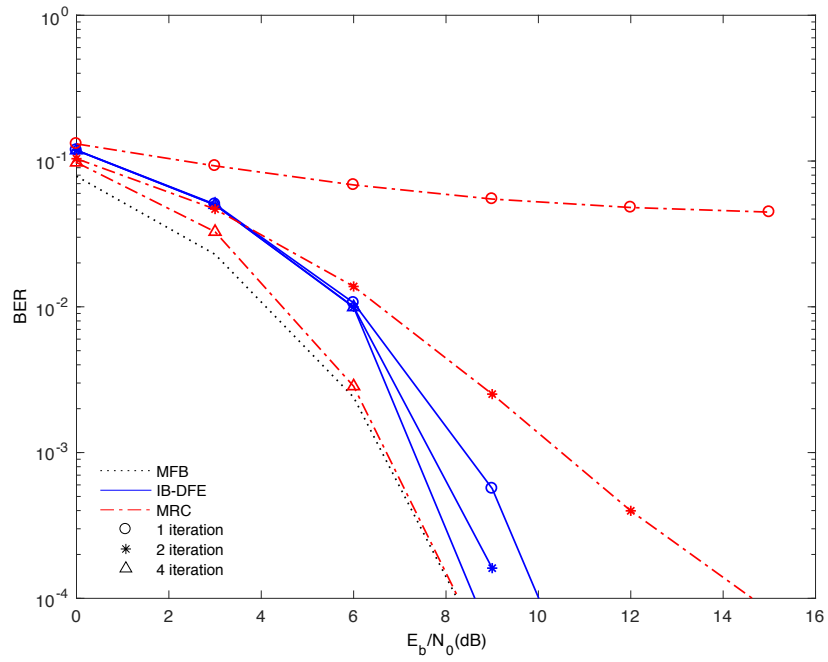


FIGURE 4.8: BER performance for IB-DFE and MRC receivers with  $P = 60$  MTs and  $R = 180$  BSs.

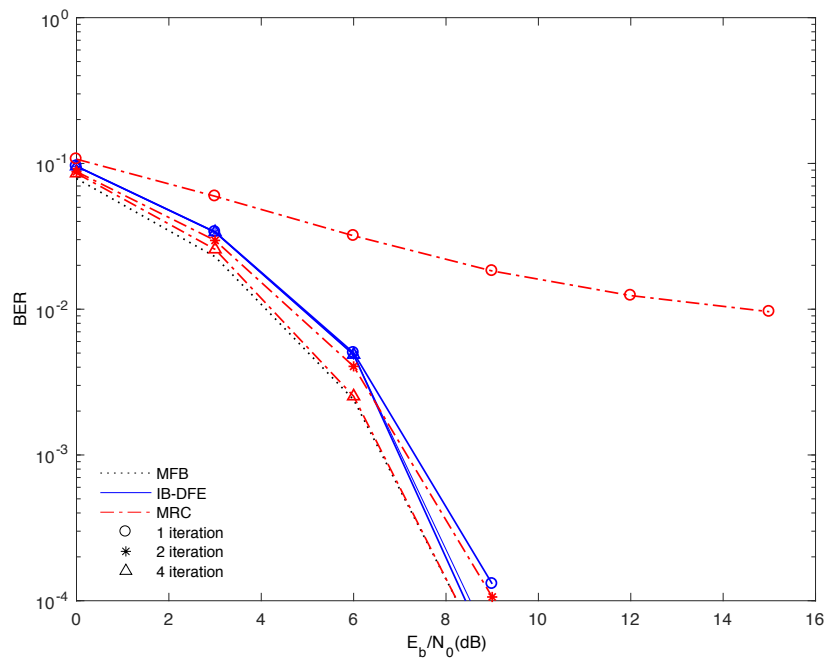


FIGURE 4.9: BER performance for IB-DFE and MRC receivers with  $P = 60$  MTs and  $R = 360$  BSs.

of the IB-DFE results in a performance curve that is only 0.3 dB away from the MFB.

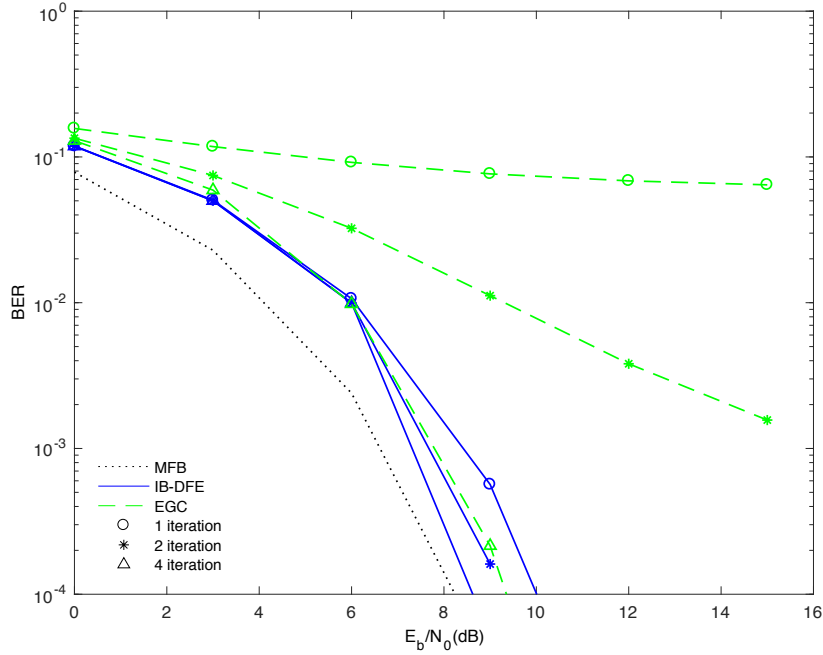


FIGURE 4.10: BER performance for IB-DFE and EGC receivers with  $P = 60$  MTs and  $R = 180$  BSs.

When  $R/P = 6$ , Fig. 4.11, the  $2^{nd}$  iteration of the EGC provides slightly better results than the previous case and the  $4^{th}$  iteration results in the performance level achieved by the  $1^{st}$  iteration of the IB-DFE. The  $2^{nd}$  and  $4^{th}$  iterations lead to substantially coincident results and for a  $BER = 10^{-4}$  the distance from the MFB is about 0.2 dB.

In these scenarios, despite the complexity of the IB-DFE, the performance achieved is higher than that of the EGC.

When comparing the two low complexity receivers, as in figures 4.12 and 4.13, it is noticeable that the first two iterations of both receivers lead to very poor results when  $R/P = 3$ , as seen in Fig. 4.12,. While the  $4^{th}$  iteration of the MRC achieves the best results coinciding with the performance of the MFB, the  $4^{th}$  iteration of the EGC stays 1 dB away.



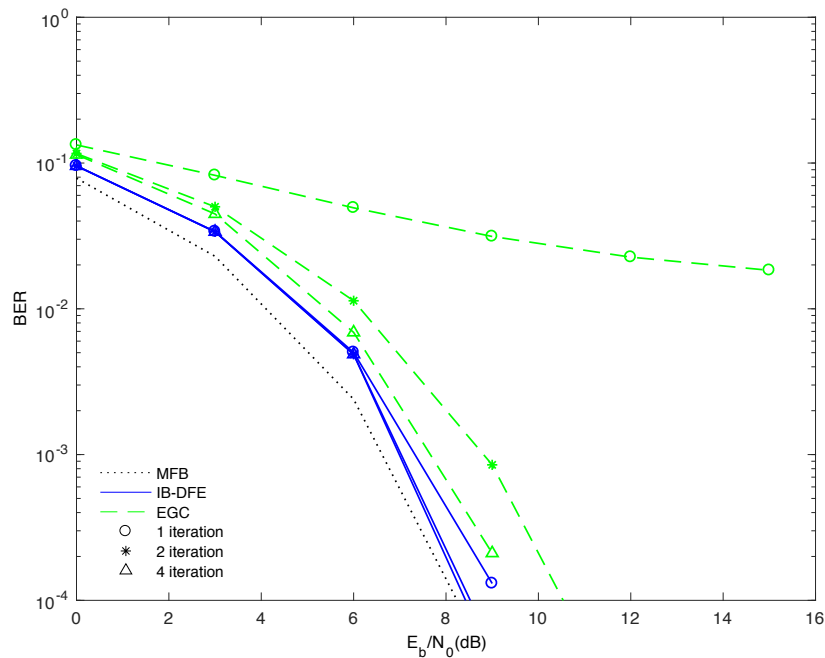


FIGURE 4.11: BER performance for IB-DFE and EGC receivers with  $P = 60$  MTs and  $R = 360$  BSs.

For the case of  $R/P = 6$ , Fig. 4.13, the performance of both receivers improve and the performance resulting from the 2<sup>nd</sup> iteration of the MRC is better than that of the 4<sup>th</sup> iteration of the EGC.

Figures 4.12 and 4.13 show us that the IB-DFE receiver presents a good performance as practically all its iterations are close to the MFB. However, it has the disadvantage of being too complex in its implementation for massive MIMO systems.

When considering a receiver of low complexity, like the MRC, and although the first two iterations do not reach a good results, the performance reached after only 4 iterations already coincides with that of the MFB and this is better than the performance achieved by IB-DFE for the same case study.

It can also be concluded that with the increase of  $R/P$  the performance of low complexity receivers improves.

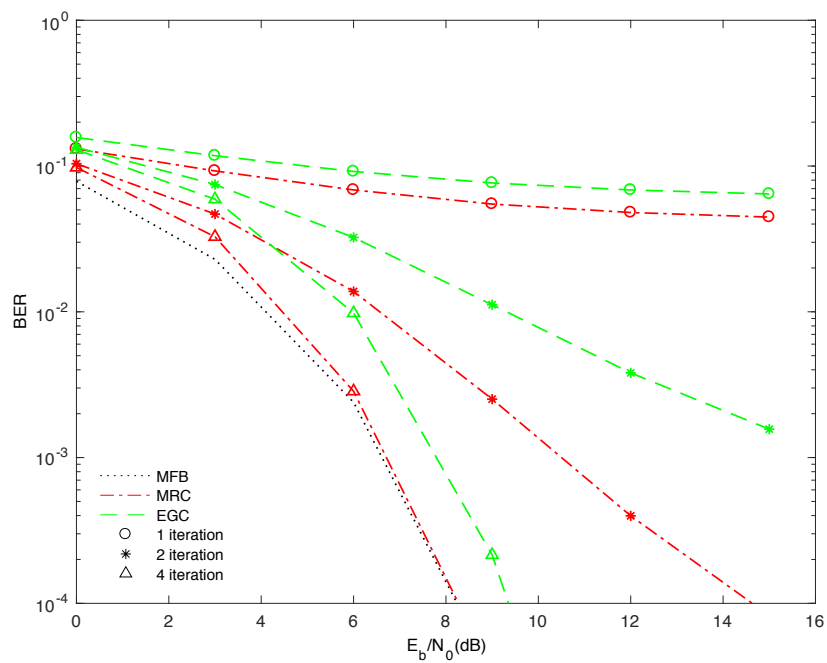


FIGURE 4.12: BER performance for MRC and EGC receivers with  $P = 60$  MTs and  $R = 180$  BSs.

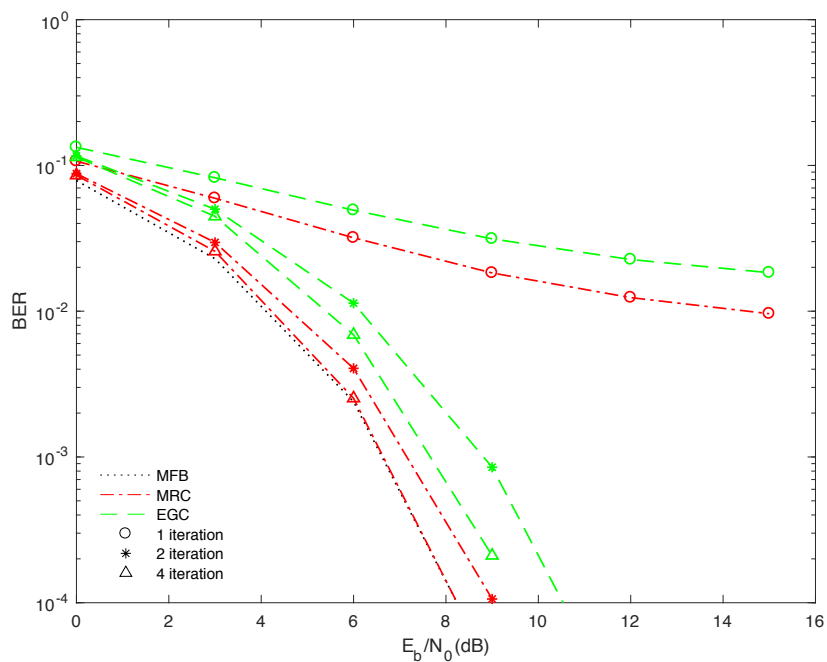


FIGURE 4.13: BER performance for MRC and EGC receivers with  $P = 60$  MTs and  $R = 360$  BSs.

## 4.4 The proposed receiver

The simplicity of implementation of the low complexity receivers allows their use in the massive MIMO systems and thus enabling its implementation for the 5G system. However, the performance of these receivers when using only one iteration is very poor. In order to use this receiver for massive MIMO systems it is then necessary to improve the efficiency of the first iteration.

The idea behind the proposed receiver is to improve the effect of the first iteration in order to be able to use low complexity receivers and still achieve a good overall system performance.

The proposed receiver [34] uses the IB-DFE in its first iteration to obtain a good performance and the MRC in the remaining iterations so that the complexity of the receiver allows its use in massive MIMO systems. The proposed receiver scheme is shown in Fig. 4.14.

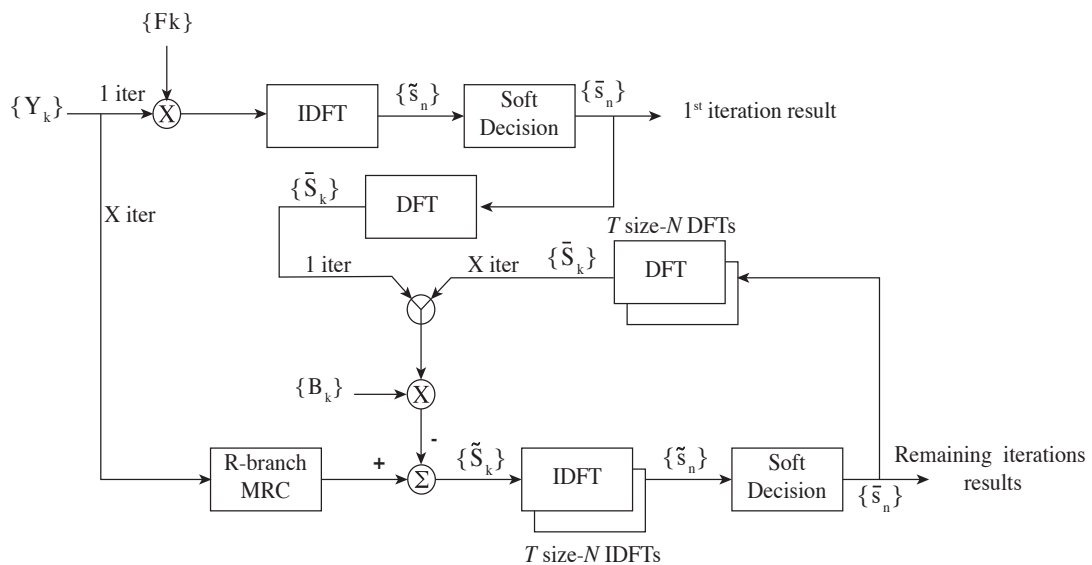


FIGURE 4.14: Proposed receiver.

In the first iteration, the proposed receiver behaves as the IB-DFE receiver, so  $\tilde{S}_{k,p}^{(1)}$  is given by:

$$\tilde{\mathbf{S}}_{k,p}^{(1)} = \mathbf{F}_{k,p}^{(1)T} \mathbf{Y}_k - \mathbf{B}_{k,p}^{(1)T} \tilde{\mathbf{S}}_{k,p}^{(0)}, \quad (4.5)$$

where  $\mathbf{F}_{k,p}^{(1)T} = [F_{k,p}^{(1,1)}, \dots, F_{k,p}^{(1,R)}]$  and  $\mathbf{B}_{k,p}^{(1)T} = [B_{k,p}^{(1,1)}, \dots, B_{k,p}^{(1,P)}]$  with

$$F_{k,p}^{(1)} = \frac{H_{k,p}^*}{\frac{1}{SNR} + (1 - (\rho^{(0)})^2) |H_{k,p}|^2}, \quad (4.6)$$

and

$$B_{k,p}^{(1)} = \rho^{(0)} (F_k^{(1)} H_k - 1). \quad (4.7)$$

As in the first iteration,  $\rho = 0$  then equations 4.6 and 4.7 can be simplified to

$$F_{k,p}^{(1)} = \frac{H_{k,p}^*}{\frac{1}{SNR} + |H_{k,p}|^2}, \quad (4.8)$$

$$B_{k,p}^{(1)} = 0. \quad (4.9)$$

So  $\tilde{\mathbf{S}}_{k,p}^{(1)}$  comes

$$\tilde{\mathbf{S}}_{k,p}^{(1)} = \mathbf{F}_{k,p}^{(1)T} \mathbf{Y}_k. \quad (4.10)$$

Using the IB-DFE in the first iteration, the resulting BER performance is good, as already studied in the previous chapters, however this type of receiver is too complex to be used for the remaining iterations.

Therefore, it is proposed that in the following iterations the receiver uses the MRC principle, which is a low complexity receiver. So, for these iterations  $\tilde{\mathbf{S}}_k^{(i)}$  is given by:

$$\tilde{\mathbf{S}}_k^{(i)} = \Psi \mathbf{H}_k^H \mathbf{Y}_k - \mathbf{B}_k^{(i)} \tilde{\mathbf{S}}_k^{(i-1)}, \quad (4.11)$$

where, as presented in section 3.3,  $\Psi$  represents the diagonal of the matrix whose element  $(p, p)^{th}$  is given by expression 4.12 and the calculation of matrix  $\mathbf{B}_k^{(i)}$  is represented in equation 4.13.

$$\left( \sum_{k=0}^{N-1} \sum_{r=1}^R |\mathbf{H}_k^{(r,p)}|^2 \right)^{-1}, \quad (4.12)$$

$$\mathbf{B}_k^{(i)} = \Psi \mathbf{H}_k^H \mathbf{H}_k - \mathbf{I}. \quad (4.13)$$

The  $\bar{\mathbf{S}}_k^{(i)}$  element present in expression 4.11 represents the average of the values resulting from the previous iteration. In the case of the proposed receiver, in the second iteration, this element is the output of the first iteration, that is, the output of the IB-DFE receiver. In the remaining iterations that element is derived from the MRC receiver.

## 4.5 Results

In this section we present the results obtained experimentally for the proposed receiver. In spite of being a receiver designed for massive MIMO systems, the BER performance achieved for a MIMO system is initially presented in Fig. 4.15.

The BER performance of the receiver with only one iteration does not match the performance of the MFB, being about 0.7 dB away. With the second and fourth iterations, values are very similar and the BER =  $10^{-4}$  is reached for  $\frac{Eb}{No} = 9$  dB.

After reviewing the performance of the proposed receiver for a MIMO system, the receiver performance for the massive MIMO systems is now analyzed.

In Fig. 4.16 we consider 60 MTs and 180 BSs and in Fig.4.17 120 MTs and 360 BSs are considered, both with  $R/P = 3$ . In these two cases the system performance is quite similar and in the first iteration, for both cases when  $\frac{Eb}{No} \approx 10$  dB, we already have a BER performance of  $10^{-4}$ .

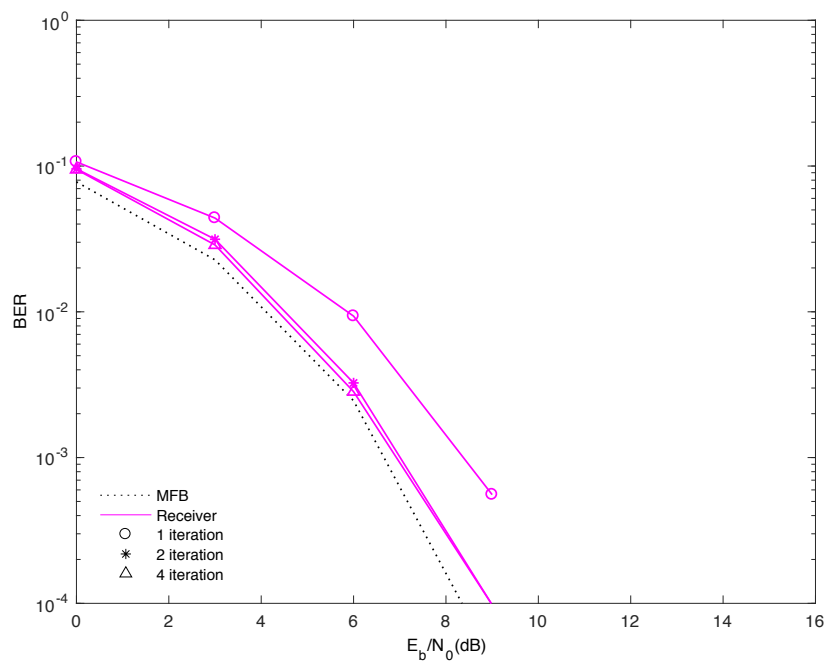


FIGURE 4.15: BER performance for the proposed receiver with  $P = 2$  MTs and  $R = 6$  BSs.

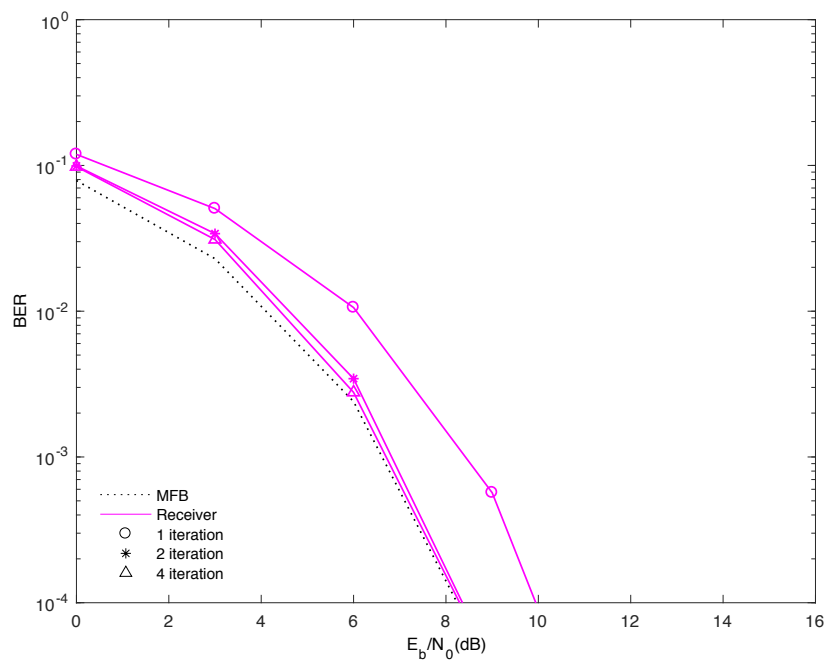


FIGURE 4.16: BER performance for the proposed receiver with  $P = 60$  MTs and  $R = 180$  BSs.

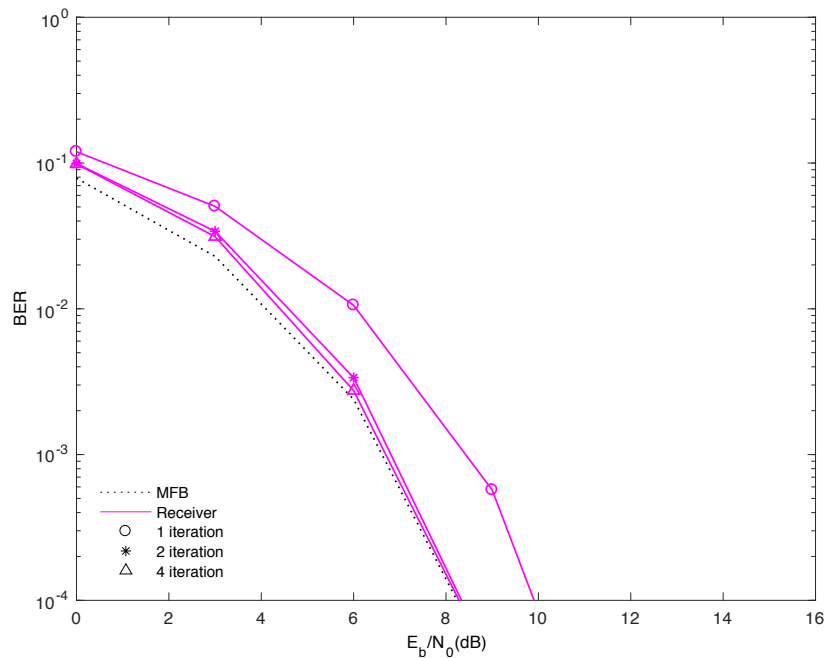


FIGURE 4.17: BER performance for the proposed receiver with  $P = 120$  MTs and  $R = 360$  BSs.

When the second and fourth iterations are applied and for  $\frac{E_b}{N_0} > 6$  dB, the performance practically coincides with that of the MFB. While the MFB reaches a BER =  $10^{-4}$  when  $\frac{E_b}{N_0} = 8.24$  dB, the proposed receiver, in its fourth iteration, reaches the same BER performance when  $\frac{E_b}{N_0} = 8.3$  dB, which, in practical terms, is equivalent.

These results allow us to conclude that despite the numbers of MTs and BSs may vary, the performance achieved is similar, provided we keep the  $R/P$  ratio for a massive MIMO.

In the last two test cases presented we used a  $R/P = 4$ ,  $P = 120$  and  $R = 480$ , as shown in Fig. 4.18 and  $R/P = 6$  ( $P = 60$  and  $R = 360$ ) as shown in Fig. 4.19.

When  $R/P = 4$ , it is possible to verify that with the increase of BSs the performance is also improved. In this case, the second and fourth iterations give the same results and from  $\frac{E_b}{N_0} = 6$  dB its performance overlaps with the performance of the MFB. The first iteration of the proposed receiver reaches a BER =  $10^{-4}$  for

$\frac{E_b}{N_0} = 9.4$  dB and the second iteration of our receiver already coincides with the MFB performance.

With the increase of  $R/P$  to 6, the first iteration of the receiver improves its performance but the following iterations present the same performance achieved for  $R/P = 4$ .

It can then be concluded that the proposed receiver performance for massive MIMO systems is excellent since its second iteration coincides with the performance of the MFB. Besides this excellent performance achieved by the receiver, its level of complexity is kept low, as explained in the previous section.

Another conclusion is that the performance of the proposed receiver improves substantially with the increase of  $R/P$ , up to a value of 4.

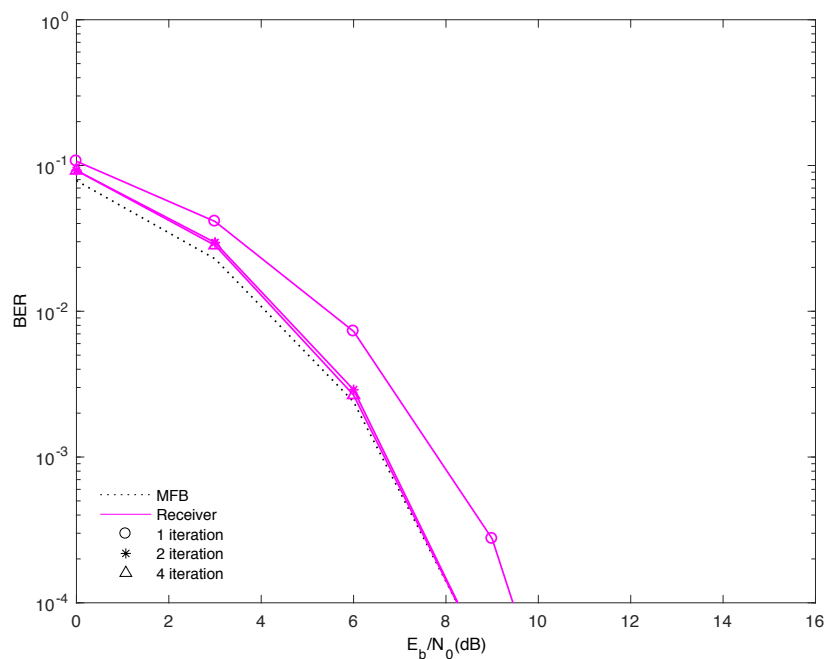


FIGURE 4.18: BER performance for the proposed receiver with  $P = 120$  MTs and  $R = 480$  BSs.



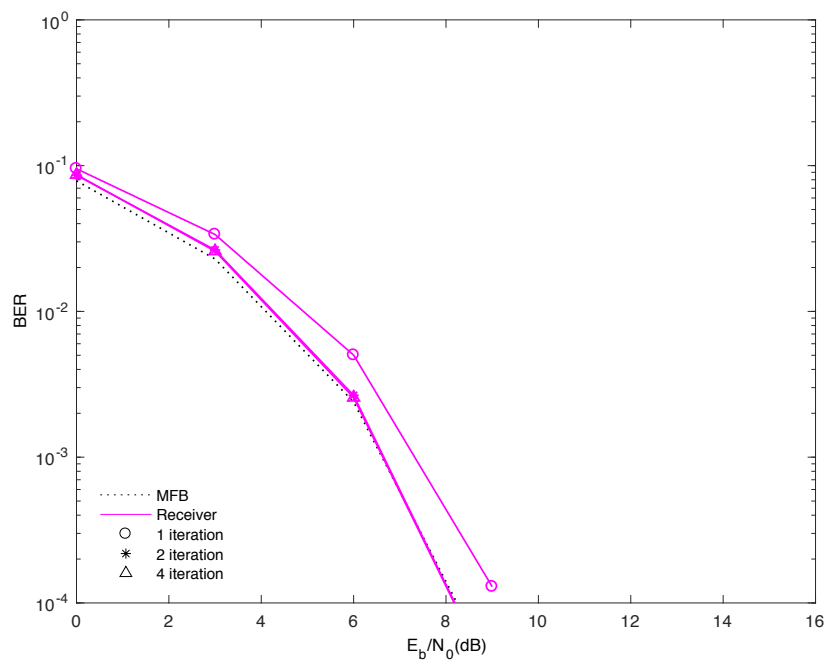


FIGURE 4.19: BER performance for the proposed receiver with  $P = 60$  MTs and  $R = 360$  BSs.



# Chapter 5

## Conclusions and Future Work

### 5.1 Conclusions

The main objective of this dissertation was to analyze the receivers used for massive MIMO systems and to present a solution for a new receiver in the frequency domain that presents low complexity and excellent performance, applicable in the new 5G system.

Initially, in chapter 2, the main differences between multicarrier and single-carrier modulations were presented and it was concluded that in order to reduce the energy expended by the MTs, the SC-FDE modulation should be used in the uplink, since this modulation transfers the complexity of the emitter to the receiver located at the BSs. Also in this chapter the transmission scheme of the iterative receiver IB-DFE was presented and it was verified that its performance approached the MFB. Finally, the MIMO and massive MIMO systems were studied.

In chapter 3, the concept of the IB-DFE receiver was extended to massive MIMO systems together with its performance analysis. It was verified that the performance achieved by MIMO and massive MIMO systems was similar and did not vary with the increase in the  $R/P$  ratio. Later on, the linear versions of the ZF, MRC and EGC receivers were presented. In the case of the ZF receiver, the performance achieved was equivalent to the first iteration of the IB-DFE,

and similarly, the ZF receiver needs matrix inversions for the estimation of the received signal. In the case of low complexity receivers with MRC and EGC, it was concluded that the performance achieved was very poor.

Finally, in chapter 4, low complexity MRC and EGC receivers were initially explained, in their iterative versions. When studying the performance achieved by these receivers, it was concluded that the performance achieved by the MRC was better than that of the EGC, for the same conditions. It was also concluded that with an increase of  $R/P$  the performance achieved improved and that after 3 iterations the MRC receiver reached the performance of the MFB. In this chapter a comparison was made between all the iterative receivers presented previously and it was demonstrated that with an increase of  $R/P$  the performance of all receivers improved. Although the first iteration of the MRC receiver did not provide good results, the fourth iteration reached the performance of the MFB. Also in this chapter, in order to fulfill the proposed objective, a receiver was proposed that in its first iteration, functioned as an IB-DFE receiver, keeping its performance and complexity, but for the remaining iterations it used the MRC receiver, thus reducing the overall complexity. When studying the performance of the proposed receiver it was verified that it was better for massive MIMO systems and that up to an  $R/P$  value of 4, in our experiments, its performance was improved. A final conclusion about the performance achieved with the proposed receiver is that, from the second iteration on, its performance coincides with the ideal performance of the MFB, but achieved with a structure of low complexity.

## 5.2 Future Work

The area of telecommunications is in constant development and although this dissertation presents a new receiver that can be used in massive MIMO systems and thus enabling the 5G system, there are several aspects that were not considered and as such can serve as a basis for future work:

- **Synchronization issues**

In this work perfect synchronism was considered between the transmitted blocks and also perfect knowledge of the channel. In the future, the impact of errors in channel estimation and synchronization should be studied. Another study that may be carried out in the future is the impact of non-linearities of amplifiers.

- **Extension for downlink**

As the MTs can not share information among themselves it would be interesting to extend the case studied for the downlink scenario using OFDM modulation.

- **Theoretical analysis**

In the future, the theoretical performance of the receivers presented can be calculated and compared with the simulated performance achieved.



# Appendices





# Appendix A

## Publications

The articles submitted for international conferences on Telecommunications are presented in this appendix.





Available online at [www.sciencedirect.com](http://www.sciencedirect.com)

**ScienceDirect**

Procedia Computer Science 109C (2017) 305–310

---

---

**Procedia**

Computer Science

---

---

[www.elsevier.com/locate/procedia](http://www.elsevier.com/locate/procedia)

The 8th International Conference on Ambient Systems, Networks and Technologies  
(ANT 2017)

## Iterative Receiver Combining IB-DFE with MRC for Massive MIMO Schemes

Daniel Fernandes<sup>a,\*</sup>, Francisco Cercas<sup>a,b</sup>, Rui Dinis<sup>b,c</sup>

<sup>a</sup>ISCTE-IUL, Av. das Forças Armadas, Lisbon, Portugal

<sup>b</sup>Instituto de Telecomunicações, Av. Rovisco Pais, 1, Lisbon, Portugal

<sup>c</sup>FCT-UNL, Campus de Caparica, Caparica, Portugal

---

### Abstract

Once we are moving to the 5G system it is imperative to reduce the complexity of massive MIMO (Multiple-Input, Multiple Output) receivers. This paper considers the uplink transmission using massive MIMO combined with SC-FDE (Single-Carrier with Frequency-Domain Equalization). We propose an iterative frequency-domain receiver merging IB-DFE (Iterative Block Decision-Feedback Equalizer) with MRC (Maximal Ratio Combining). We propose a novel approach to reduce the complexity of the receiver by avoiding matrix inversions while maintaining a level of performance very close to the Matched Filter Bound (MFB), which makes it an excellent option for 5G systems.

1877-0509 © 2017 The Authors. Published by Elsevier B.V.  
Peer-review under responsibility of the Conference Program Chairs.

*Keywords:* Massive MIMO; 5G; SC-FDE; IB-DFE; MRC

---

### 1. Introduction

The 5<sup>th</sup> Generation imposes high quality of service at high bit rates. This requests can be fulfilled, in part, with MIMO. In fact, when we speak about MIMO it is well know that while the spectral efficiency of the system is improved also its complexity increases<sup>1</sup>. Yet, despite this, we can raise the number of antenna elements to tens or even hundreds leading to massive MIMO.

As shown in<sup>2</sup> massive MIMO schemes are expected to be the central elements of future 5G systems, therefore it is desirable that we use simple techniques at the receiver side.

In order to improve an efficient power amplification at the mobile terminals (MTs) we use SC-FDE for the uplink transmission once single-carrier signals have much lower envelope fluctuations than OFDM (Orthogonal Frequency Division Multiplexing) ones<sup>3</sup>.

When we want to reach MFB the main receiver used was based on iterative frequency-domain, for instance, IB-DFE can be used to achieve MFB with just a few iterations. The IB-DFE receiver was proposed in<sup>4</sup> and its performance

---

\* Corresponding author.  
E-mail address: [dfsfs@iscte-iul.pt](mailto:dfsfs@iscte-iul.pt)

was studied in several articles such as<sup>5,6</sup>. On one hand we have the excellent performance that IB-DFE brings but on the other hand we have the complexity resulting from the matrix inversions.

As we know, in massive MIMO schemes the number of antenna elements is high leading to large matrices, consequently the matrix inversions are complex operations<sup>7</sup>. The MRC receiver does not require matrix inversions therefore its complexity is decreased, although the interference among different transmitted streams and the inter-symbol interference (ISI) increases.

In this paper we propose an iterative frequency-domain receiver that only demands matrix inversions in the first iteration, resulting in a low-complexity receiver with an extraordinary performance.

This paper is organized as follows: in Section II we describe the adopted system, following to Section III where we present the first iteration of the receiver design and the remaining iterations. Section IV presents a set of performance results and in section V we conclude this paper.

Through the paper we employ the following notation: vectors and matrices are denoted by upper-case, italic, bold letters,  $\mathbf{X}^T$  and  $\mathbf{X}^H$  denotes the Transpose and Hermitian of the matrix  $\mathbf{X}$ . The expectation of  $x$  is denoted by  $\mathbb{E}[x]$ .

### 1.1. Research objectives

This work intends to develop a low complexity receiver that allows to achieve a high level of performance suitable for the 5G system. The low complexity achieved is due to the fact that matrix inversions are not used in our algorithm except at first iteration, as opposed to most common approaches.

## 2. System characterization

For this work we consider an uplink single-carrier massive MIMO scenario presented in Fig. 1 where  $T$  MT (Mobile Terminals) are communicating with a base station (BS). In this case a BS has  $R$  receive antennas with  $R \gg T$ . In order to simplify the scenario we only consider a single antenna for the MT, with no loss of generality.

We use SC-DFE modulations in MT and perfect synchronization and channel estimation in the receiver are assumed. Once we use SC-FDE, in the transmission side, for each transmitted block of  $N$  data symbol a cyclic prefix longer than the maximum overall channel impulse response is appended and in the receiver side this prefix is removed.

The data block transmitted in the  $t^{\text{th}}$  MT is  $\{x_n^{(t)}; n = 0, 1, \dots, N - 1\}$  with  $x_n^{(t)}$  selected from a given constellation (in our case we consider QPSK constellation) according to the Gray mapping rule. The received block at the  $r^{\text{th}}$  BS, after we remove the prefix, is  $\{y_n^{(r)}; k = 0, 1, \dots, N - 1\}$  and the corresponding frequency-domain block is  $\{Y_k^{(r)}; k = 0, 1, \dots, N - 1\}$ .

The block  $Y_n^{(r)}$ , when expressed in matrix form, is represented by:

$$\mathbf{Y}_k^{(r)} = [Y_k^{(1)}, \dots, Y_k^{(R)}]^T = \mathbf{H}_k \mathbf{X}_k + \mathbf{N}_k \quad (1)$$

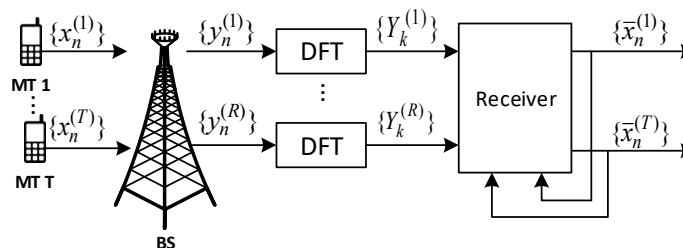


Fig. 1. System model.

where  $\mathbf{H}_k$  is the  $\mathbf{R} \times \mathbf{T}$  channel matrix for the  $k^{\text{th}}$  frequency,  $\mathbf{X}_k = [X_k^{(1)}, \dots, X_k^{(T)}]^T$  and  $\mathbf{H}_k$  denotes the channel noise. It is also assumed that  $\mathbb{E}[\mathbf{N}_k \mathbf{N}_k^H] = N_0 \mathbf{I}_R$ .

### 3. Receiver Structure

In this paper we propose a low-complexity iterative frequency-domain receiver. Due to its low complexity this receiver is indicated for massive MIMO schemes. Once complexity is mainly related with the matrix inversions we will try to simplify the receiver by rendering this operation.

Therefore we propose a receiver that uses a linear decision feedback equalizer, in our case we use IB-DFE in the first iteration, and on the following iterations it uses a structure that does not involve matrix inversions, the MRC technique.

This combination was chosen because the results of the first iteration of the MRC are far from MFB. So, if we start with the IB-DFE and use the resulting values to initiate the MRC receiver in the first iteration (the second in the global) than it will be very close to the MFB.

#### 3.1. First iteration

The conventional IB-DFE receiver is well studied in<sup>4,5</sup> and<sup>8</sup>.

As we can see in the mentioned papers, the complexity of the receiver is related to the need of solving a system of  $R$  equations for every frequency of each MT. In the first iteration, if we look for the  $p^{\text{th}}$  MT, the estimated symbols  $\{\tilde{x}_n^{(p)}; n = 0, 1, \dots, N - 1\}$  are the hard decisions of the time-domain detector output  $\{\tilde{x}_n^{(p)}; n = 0, 1, \dots, N - 1\} = \text{IDFT}\{\tilde{\mathbf{X}}_k^{(p)}; k = 0, 1, \dots, N - 1\}$ , where IDFT denotes the Inverse Discrete Fourier Transform.

The  $\tilde{\mathbf{X}}_k^{(p)}$  is given by:

$$\tilde{\mathbf{X}}_k^{(p)} = \mathbf{F}_k^{(p)T} \mathbf{Y}_k^Q - \mathbf{B}_k^{(p)T} \tilde{\mathbf{X}}_k^{(p)} \quad (2)$$

where  $\mathbf{F}_k^{(p)T} = [F_k^{(p),(1)}, \dots, F_k^{(p),(R)}]^T$  represents the feedforward coefficients and  $\mathbf{B}_k^{(p)T} = [B_k^{(p),(1)}, \dots, B_k^{(p),(P)}]^T$  denotes the feedback coefficients.  $\tilde{\mathbf{X}}_k^{(p)}$  represents the average values conditioned to the detector output calculated in<sup>8</sup>. At the first iteration there are no feedback coefficients so the equation 3 can be simplified to:

$$\tilde{\mathbf{X}}_k^{(p)} = \mathbf{F}_k^{(p)T} \mathbf{Y}_k^Q \quad (3)$$

The IB-DFE receiver for the first iteration is presented in Fig. 2.

#### 3.2. Remaining iterations

As previously stated, the IB-DFE is very complex and the first iteration of the MRC has a poor performance, so we decided to use the output of IB-DFE (in the first iteration) to improve the performance of the MRC (Fig. 3).

Another advantage of the MRC receiver, besides its low complexity for the system, is the small correlation between channels and between different transmitters and receive antennas. In fact, the elements outside main diagonal  $\mathbf{A}_k^H \mathbf{H}_k$

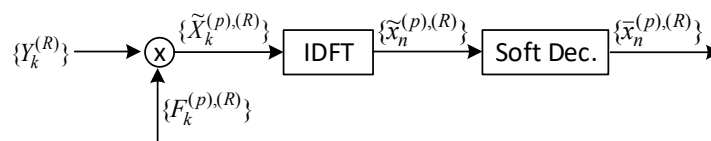


Fig. 2. IB-DFE receiver for the first iteration

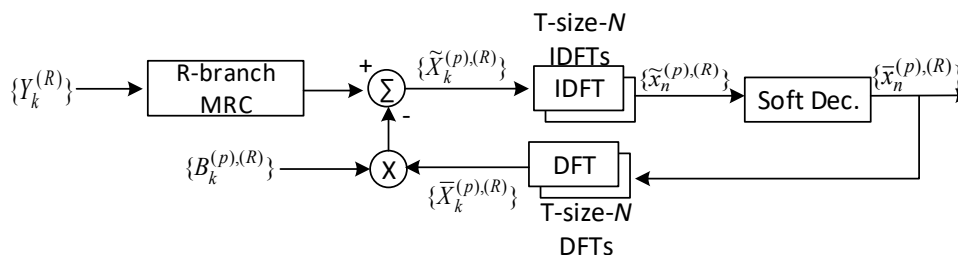


Fig. 3. Remaining iterations with MRC

are much lower than the ones at its diagonal<sup>9</sup>. The matrix  $A$  is given by:

$$[A]_{i,i'} = [H]_{i,i'} \tag{4}$$

As carefully explained in<sup>9</sup> to the SC-FDE, we employ a receiver based on  $A_k^H Y_k$  but the residual interference levels are still considerable, so we propose a receiver where

$$\bar{X}_k = \Psi A_k^H Y_k - B_k \bar{X}_k, \tag{5}$$

the diagonal matrix, whose  $(t, t)^{th}$  element is given by  $(\sum_{k=0}^{N-1} \sum_{r=1}^R |H_k^{(r,t)}|^2)^{-1}$  is represented by  $\Psi$ . This element ensures that the overall frequency-response for each MT of the “channel plus receiver” has average 1<sup>6</sup>.

$B_k$  is used to remove the residual ISI and inter-user interference.

$\bar{X}_k$  is used to canal interference and its values are conditioned with the previous iterations.

#### 4. Results

In this section, we consider the proposed receiver and present a set of performance results. We consider a massive MIMO system with  $T=4$  single-antenna transmitter with  $R$  receivers. We also consider the uplink scenario with SC-FDE modulations implemented in each antenna. Each block has  $N=256$  data symbols, each symbol is selected from a QSPK constellation, plus an appropriate CP. Every channel has 100 slots, symbol-spaced, equal-power multipath components.

We consider an uncorrelated Ryeligh channel with different links between transmit and receive antennas. It is assumed perfect synchronization and channel estimation. In this simulations we assume a BS with  $R=16$  or  $R=32$  receive antennas and 4 iterations.

First in Fig. 4 we present the performance of the IB-DFE receiver. As we can see the performance of this receiver never matches with MFB. After the first iteration the remaining iterations have about the same performance as the first one for an error rate above  $5 \times 10^{-2}$  for  $R=16$  and  $10^{-2}$  for  $R=32$ .

The performance of a receiver that does not require matrix inversions is present in Fig. 5. In this figure it is possible to see that for both  $R=16$  and  $R=32$  the first two iterations are far away from the MFB but the remaining iterations approach it.

In Fig. 6 we can see the performance of the implemented receiver. We can see in first iteration the performance of IB-DFE and in the remaining iterations the performance of the MRC. In fact, the junction of this two receivers improves the performance, after the first iteration. This receiver approaches MFB with only 2 iterations and merely needs matrix inversions in the first iteration.

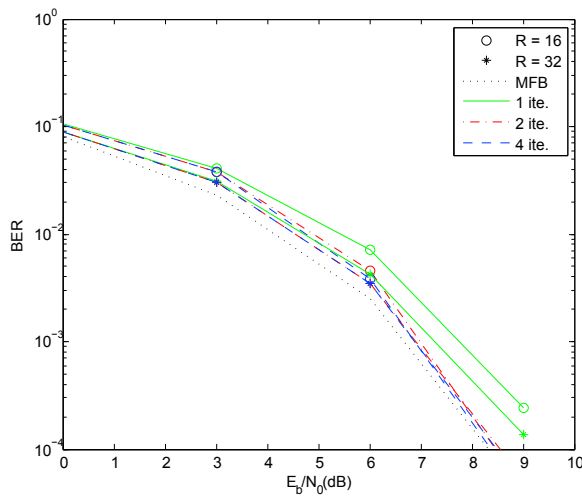


Fig. 4. BER performance for IB-DFE receiver

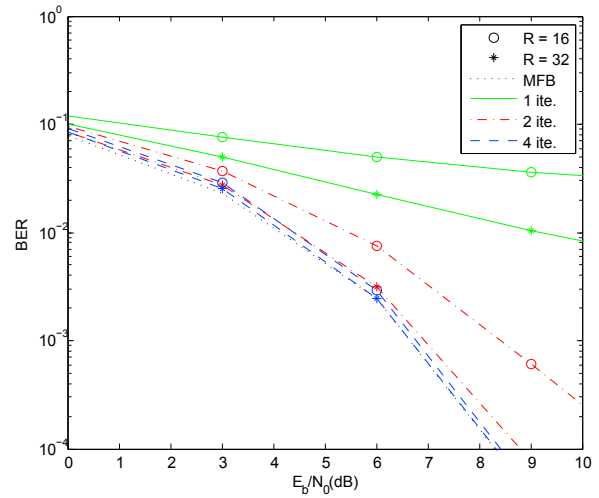


Fig. 5. BER performance for MRC receiver

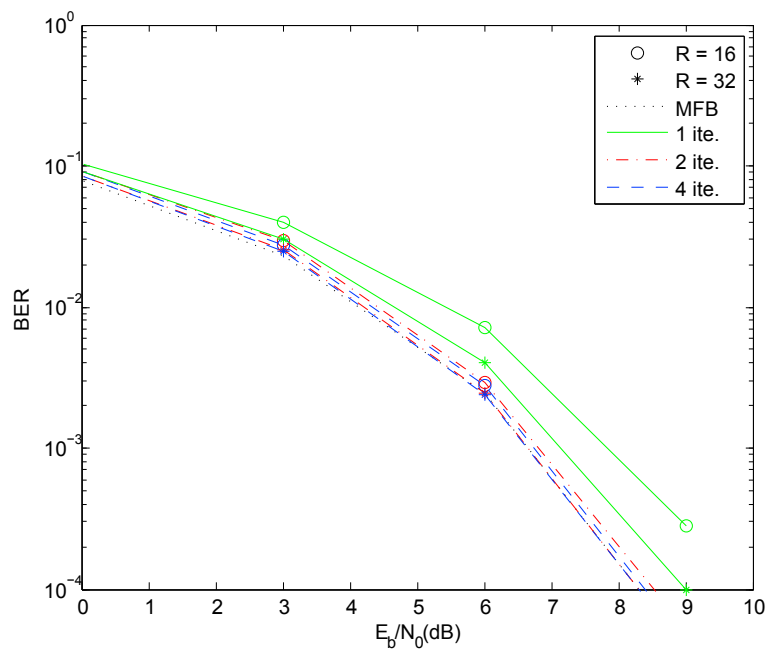


Fig. 6. BER performance for the proposed receiver

## 5. Conclusion

In this paper a low complexity iterative receiver was proposed. This receiver was designed for massive MIMO schemes and after the second iteration the results are already very close to the MFB. The greatest advantage of this

receiver proposal is the fact that it only needs one matrix inversion and no matrix inversions are used at remaining iterations.

With this research work it can be shown that it is possible to reduce the complexity of the receiver by maintaining high performance levels. These excellent performance results are very promising for the future of 5G system, as it is expected to achieve high performance with low complexity, as proposed by our algorithm, enabling cheaper and more efficient receivers.

### **Acknowledgements**

This work was partially supported by Fundação para a Ciência e Tecnologia (FCT) under the project PEst-OE/EEI/LA0008/2013.

### **References**

1. F. Rusek, D. Persson, Buon Kiong Lau, E. G. Larsson, T. L. Marzetta, F. Tufvesson, Scaling Up MIMO: Opportunities and Challenges with Very Large Arrays, *IEEE Signal Processing Magazine* 30 (1) (2013) 40–60.
2. F. Boccardi, R. Heath, A. Lozano, T. Marzetta, P. Popovski, Five disruptive technology directions for 5G, *IEEE Communications Magazine* 52 (2) (2014) 74–80.
3. D. Falconer, S. Ariyavisitakul, A. Benyamin-Seeyar, B. Eidson, Frequency domain equalization for single-carrier broadband wireless systems, *IEEE Communications Magazine* 40 (4) (2002) 58–66.
4. N. Benvenuto, S. Tomasin, Block iterative DFE for single carrier modulation, *Electronics Letters* 38 (19) (2002) 1144–1145.
5. N. Benvenuto, R. Dinis, D. Falconer, S. Tomasin, Single Carrier Modulation With Nonlinear Frequency Domain Equalization: An Idea Whose Time Has Come-Again, *Proceedings of the IEEE* 98 (1) (2010) 69–96.
6. R. Dinis, R. Kalbasi, D. Falconer, A. Banihashemi, Iterative Layered Space-Time Receivers for Single-Carrier Transmission Over Severe Time-Dispersive Channels, *IEEE Communications Letters* 8 (9) (2004) 579–581.
7. R. Dinis, P. Carvalho, D. Borges, LOW COMPLEXITY MRC AND EGC BASED RECEIVERS FOR SC-FDE MODULATIONS WITH MASSIVE MIMO SCHEMES, *IEEE Global Conf. on Signal and Information Processing - Global SIP 1* (2016) 1–4.
8. F. Ribeiro, R. Dinis, F. Cercas, A. Silva, Receiver design for the uplink of base station cooperation systems employing SC-FDE modulations, *EURASIP Journal on Wireless Communications and Networking* 2015 (1) (2015) 7.
9. P. Montezuma, R. Dinis, Iterative receiver based on the EGC for massive MIMO schemes using SC-FDE modulations, *Electronics Letters* 52 (11) (2016) 972–974.



# Efficient Frequency-Domain Detection for Massive MIMO Systems

Lorenzo Cabral<sup>(1)</sup>, Daniel Fernandes<sup>(1)</sup>, Francisco Cercas<sup>(1,2)</sup>, Rui Dinis<sup>(2,3)</sup>

<sup>(1)</sup> ISCTE-IUL, Av. das Forças Armadas, Lisbon, Portugal

<sup>(2)</sup> Instituto de Telecomunicações, Av. Rovisco Pais, 1, Lisbon, Portugal

<sup>(3)</sup> FCT-UNL, Campus de Caparica, Caparica, Portugal

**Abstract**—Reduced-complexity implementations are critical for massive MIMO (Multiple Input, Multiple Output) systems. In this paper we consider the uplink of broadband massive MIMO systems employing SC-FDE (Single-Carrier with Frequency-Domain Equalization) schemes, where multiple users transmit to a single base station with a large number of antennas. We propose low-complexity frequency-domain detection schemes that allow excellent performance, but do not require matrix inversions.

**Index Terms**—massive MIMO, 5G, SC-FDE, IB-DFE, ZF, MRC, EGC

## I. INTRODUCTION

Future 5G systems are expected to provide huge increase in the user bit rate and overall system spectral efficiency when compared with current systems [1], [2]. MIMO (Multiple Input, Multiple Output) techniques allow multiple data stream in the same physical channel, which leads to significant gains in the system's spectral efficiency (in theory, upper-bounded by the minimum between the number of transmit and receive antennas, although in practical implementations can be lower due to correlations between antennas) [3], [4].

Massive MIMO systems push the MIMO concept even further, involving tens or even hundreds of antennas, and allowing huge capacity gains. Therefore, massive MIMO schemes are expected to be central elements of future 5G systems. However, the implementation complexity can be prohibitively high, namely in terms of signal processing requirements. Therefore, massive MIMO cannot be regarded simply as a scaled version of conventional MIMO schemes. In fact, it is desirable to have massive MIMO schemes with low complexity implementations [5], [6].

The multipath propagation effects set additional difficulties for broadband systems, since the channel becomes severely time-dispersive. SC-FDE (Single-Carrier with Frequency-Domain Equalization) is recognized as a promising technique for the uplink transmission since the frequency-domain receiver implementation makes it suitable for severely time-dispersive channels and the transmitted signals have much lower envelope fluctuations than OFDM (Orthogonal Frequency Division Multiplexing) signals, allowing an efficient power amplification [7], [8]. Iterative frequency-domain receivers such as the IB-DFE (Iterative Block Decision-Feedback Equalizer) [9], [10], [11] allow further performance improvements, which can be close to the MFB (Matched Filter Bound) [12]. These techniques were already shown to allow

excellent performance in MIMO systems [11]. However, the complexity associated to conventional MIMO FDE receivers in general and IB-DFE receivers in particular can be very high for large MIMO systems. This is mainly due to the need to invert large matrices.

In this paper we consider the uplink transmission of wireless systems employing SC-FDE techniques and massive MIMO schemes. We consider multiple mobile terminals transmitting simultaneously to a single base station with a large number of antennas. We propose iterative frequency-domain receivers that do not require matrix inversions.

This paper is organized as follows: We start in Section II with the description of the adopted system, following to Section III where each subsection presents one of the receiver design, beginning with Zero Forcing and ending with the EGC-based Iterative Receiver. The performance results are present in Section IV and section V concludes this paper.

Throughout this paper we employ the following notation: matrices are denoted by upper-case, bold, non-italic letters and  $\mathbb{E}(x)$  denotes the expectation of  $x$ . The transpose and Hermitian (conjugated transpose) of the matrix  $\mathbf{X}$  are  $\mathbf{X}^T$  and  $\mathbf{X}^H$ , respectively. The  $N \times N$  identity matrix is  $\mathbf{I}_N$ .

## II. SYSTEM CHARACTERIZATION

In this work we consider an uplink scenario where a Base Station (BS) equipped with  $R$  receive antennas is receiving the signals from  $T$  Mobile Terminals (MTs), as illustrated in Fig. 1. Without loss of generality, we assume that each MT has a single antenna (the generalization for the case with multiple-antenna transmitters is straightforward) and the number of receiver antennas is much higher than the number of transmit antennas (i.e.,  $R \gg T$ ). Since  $R \gg 1$  and  $T > 1$  this can be regarded as a massive MIMO scenario, at least at the receiver side.

An SC-FDE scheme is employed and we assume perfect synchronization and channel estimation at the receiver side. No channel information is required at the transmitters, but we assume that the blocks transmitted by each MT arrive perfectly aligned at the BS (in practice, this means some kind of time advance mechanism is required by the MTs, although residual timing errors can be absorbed by the cyclic prefix). The transmitted block associated to the  $t^{\text{th}}$  transmitter (i.e., the  $t^{\text{th}}$  MT,  $t = 1, 2, \dots, T$ ) is  $\{x_{n,t}; n = 0, 1, \dots, N-1\}$ , with  $N$  denoting the block size, common to all MTs, and  $x_{n,t}$  is

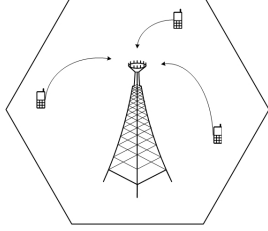


Fig. 1. Adopted uplink scenario.

selected from a given constellation. In this paper we consider QPSK modulation and Gray mapping. The corresponding frequency-domain block, i.e., its size- $N$  DFT (Discrete Fourier Transform) is  $\{X_{k,t}; k = 0, 1, \dots, N - 1\}$ .

As with other prefix-assisted block transmission techniques, a cyclic prefix longer than the maximum overall channel impulse response is appended to each block before being transmitted through a MIMO multipath channel. The received signal at the  $r^{\text{th}}$  receive antenna,  $r = 1, 2, \dots, R$ , is sampled, the cyclic prefix is removed and passed to the frequency-domain by a DFT operation leading to the block  $\{Y_{k,r}; k = 0, 1, \dots, N - 1\}$ . In matrix format, the signal associated to the  $k^{\text{th}}$  subcarrier is

$$\mathbf{Y}_k = \mathbf{H}_k \mathbf{X}_k + \mathbf{N}_k, \quad (1)$$

where  $\mathbf{Y}_k$  is a size- $R$  column vector with  $r^{\text{th}}$  element given by  $Y_{k,r}$ ,  $\mathbf{H}_k$  is the  $R \times T$  channel matrix associated to the  $k^{\text{th}}$  subcarrier,  $\mathbf{X}_k$  is a size- $T$  column vector with  $t^{\text{th}}$  element given by  $X_{k,t}$  and  $\mathbf{N}_k$  denotes the channel noise, assumed white and Gaussian, with one-sided PSD (Power Spectral Density)  $N_0$  and uncorrelated for different subcarriers and different antennas, i.e.,  $\mathbb{E}[\mathbf{N}_k \mathbf{N}_k^H] = N_0 \mathbf{I}_R$ .

### III. RECEIVERS DESIGN

Along this section we will present some receivers we can use with massive MIMO schemes. First are presented two techniques that use matrix inversion including IB-DFE. As we know an IB-DFE receiver doesn't require the channel decoder output at the feedback loop which allows to obtain high performance [13]. The fact of using matrix inversion make these techniques very complex to use with massive MIMO, consequently we explain other two techniques, that don't use matrix inversion. This four techniques are explained in detail in the following subsections.

#### A. Zero Forcing

The structure of the receiver that we are going to study is shown in Fig. 2. The signal received is then sampled at the receiver and the samples contained by the Cyclic Prefix (CP) are eliminated, leading to the time-domain samples  $\{y_n^{(r)}; n = 0, \dots, N - 1\}$ . Then a size- $N$  DFT results the corresponding frequency-domain block  $\{\mathbf{Y}_k^{(r)}; k=0, 1, \dots, N-1\}$ , with  $\mathbf{Y}_k^{(r)}$  given by [14]

$$\mathbf{Y}_k^{(r)} = [\mathbf{Y}_k^{(1)}, \dots, \mathbf{Y}_k^{(R)}]^T = \mathbf{S}_k \mathbf{H}_k + \mathbf{N}_k, \quad (2)$$

With  $\mathbf{H}_k$  denoting the  $\mathbf{R} \times \mathbf{T}$  channel matrix for  $k^{\text{th}}$  ( $k = 0, 1, \dots, N - 1$ ) frequency with  $(r,t)^{\text{th}}$  element  $\mathbf{H}_k^{(r,t)}$ ,  $\mathbf{S}_k = [\mathbf{S}_k^{(1)}, \dots, \mathbf{S}_k^{(R)}]^T$  and  $\mathbf{N}_k$  representing the frequency-domain term of the channel noise. The corresponding equalized samples are given by

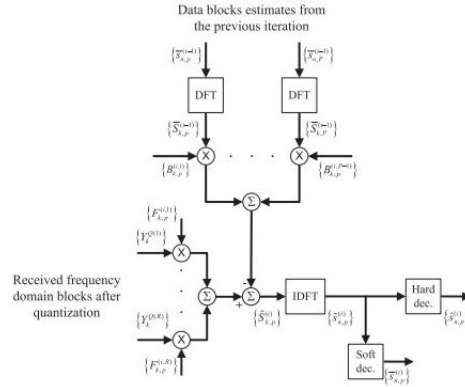
$$\tilde{\mathbf{S}}_k = \mathbf{F}_k^T \mathbf{Y}_k \quad (3)$$

It can be demonstrated that  $(\mathbf{H}^H \mathbf{H})^{-1} \mathbf{H}^H \times \mathbf{H} = \mathbf{I}$ . It is well known as Zero Forcing (ZF) criterion [15]. Therefore, after the equalizer and for a linear ZF-based receiver, the data symbols can be obtained from the IDFT of the block  $\{\tilde{\mathbf{S}}_k^{(l)}; k = 0, 1, \dots, N - 1\}$ , where

$$\tilde{\mathbf{S}}_k = [\tilde{\mathbf{S}}_k^{(1)}, \dots, \tilde{\mathbf{S}}_k^{(R)}]^T = (\mathbf{H}_k^H \mathbf{H}_k)^{-1} \mathbf{H}_k \times \mathbf{Y}_k \quad (4)$$

Under ZF criterion, the channel is fully inverted, resulting in a perfect equalized channel after the FDE. In the presence of channel noise, this inversion causes significant enhancement of the channel noise at subchannels with local deep notches, resulting in a higher Signal-to-Noise Ratio (SNR) reduction. However, in the absence of channel noise, this perfect inversion leads to exact values of the samples and avoids the last situation (see details in [16]).

#### B. IB-DFE Receivers


 Fig. 2. IB-DFE receiver structure with  $N_{Rx}$ -branch space diversity.

The need to solve a system of  $R$  equations for every frequency of each user and each, which includes a FFT/IFFT pair, at each iteration, severely conditions the complexity of these receivers. For the  $i^{\text{th}}$  iteration, the estimated symbols associated with the  $p^{\text{th}}$  MT  $\{\hat{s}_{n,p}; n = 0, 1, \dots, N - 1\}$  are the hard decisions at the output of the time-domain detector  $\{\tilde{s}_{n,p}; n = 0, 1, \dots, N - 1\} = \text{IDFT}\{\tilde{S}_{k,p}; k = 0, 1, \dots, N - 1\}$ , where  $\tilde{S}_{k,p}$  is given by:

$$\tilde{\mathbf{S}}_{k,p} = \mathbf{F}_{k,p}^T \mathbf{Y}_k^Q - \mathbf{B}_{k,p}^T \tilde{\mathbf{S}}_{k,p}; \quad (5)$$

with  $\mathbf{F}_{k,p}^T = [F_{k,p}^{(1)}, \dots, F_{k,p}^{(R)}]^T$  and  $\mathbf{B}_{k,p}^T = [B_{k,p}^{(1)}, \dots, B_{k,p}^{(P)}]^T$  represents the feedforward and feedback coefficients, respectively. Vector  $\tilde{\mathbf{S}}_{k,p}$  denotes the average values conditioned at output detector for user  $p$  of a given iteration and it can be calculated as in [16], [17].

The receiver is characterized by  $\mathbf{F}_{k,p}$  and  $\mathbf{B}_{k,p}$  ( $k=0,1,\dots,N-1$ ) coefficients, for a given iteration and detection of the  $p^{\text{th}}$  MT. These coefficients are selected in order to minimize the MSE, given by:

$$\Theta_{k,p} = \mathbb{E} [|\tilde{S}_{k,p} - S_{k,p}|^2] = \mathbb{E} [|\mathbf{F}_{k,p}^T \mathbf{Y}_k^Q - \mathbf{B}_{k,p}^T \tilde{\mathbf{S}}_{k,p} - S_{k,p}|^2]$$

as can be consulted in [18]. It can be demonstrated that the optimum values of  $\mathbf{F}_{k,p}$  and  $\mathbf{B}_{k,p}$  are [17]:

$$\mathbf{F} = \kappa \mathbf{\Lambda} \mathbf{H}^H \mathbf{e}_p, \quad (6)$$

and

$$\mathbf{B} = \alpha \mathbf{H} \mathbf{F} - \mathbf{e}_p, \quad (7)$$

with

$$\mathbf{\Lambda} = (\mathbf{H}^H (\mathbf{I}_P - \mathbf{P}^2) \mathbf{H} + \mathbf{R}_{N^{\text{Tot}}} \mathbf{R}_S^{-1} |\alpha|^{-2})^{-1}, \quad (8)$$

where  $\kappa$  is selected so that  $\gamma_p = 1$ , in order to obtain a normalized FDE with  $\mathbb{E} [\tilde{s}_{n,p}] = s_{n,p}$ ,  $\mathbf{R}_S = \mathbb{E} [\mathbf{S}^* \mathbf{S}^T] = 2\sigma_S^2 \mathbf{I}_P$  and  $\mathbf{R}_{N^{\text{Tot}}} = \mathbb{E} [\mathbf{N}^{\text{Tot}*} \mathbf{N}^{\text{Tot}T}] = |\alpha|^2 \mathbf{R}_N + \mathbf{R}_D$ , corresponding to the correlation matrices of  $\mathbf{S}$  and  $\mathbf{N}^{\text{Tot}}$ , respectively.  $\mathbf{R}_N = 2\sigma_N^2 \mathbf{I}_R$  and  $\mathbf{R}_D = 2 \text{diag}(\sigma_D^{(1)2}, \sigma_D^{(2)2}, \dots, \sigma_D^{(R)2})$  are the correlation matrices of the channel and quantization noise, respectively.  $\sigma_S^2$  and  $\sigma_N^2$  represent the symbol's variance and noise's variance, respectively with  $\mathbf{P} = \text{diag}(\rho_1, \dots, \rho_P)$ , where  $\rho_p$  denotes the correlation coefficients and represents a measure of the estimates reliability associated with the  $i^{\text{th}}$  iteration. It is given by:

$$\rho_p = \frac{\mathbb{E} [\tilde{s}_{n,p} s_{n,p}^*]}{\mathbb{E} [|\tilde{s}_{n,p}|^2]} \quad (9)$$

and can be calculated as in [16].

### C. MRC-based Iterative Receiver

Massive MIMO usually needs high dimension matrices that need to be inverted, which presents a heavy computational burden. To overcome this situation and to develop a lower complexity receiver we perform the Maximal-Ratio Combining (MRC) of the signals associated with each receiver antenna. This is a technique to combine the signals from multiple diversity branches. MRC performs the synchronization of the receiver signals and each one is multiplied by a weight factor proportional to the signal amplitude, thus offering the optimum

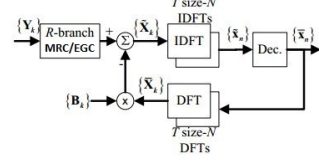


Fig. 3. IB-DFE receiver employed MRC/EGC.

value of SNR. The motivation behind this approach is that,  $\mathbf{H}^H \mathbf{H} \approx k \mathbf{I}$ , where  $\mathbf{I}$  is an identity matrix and  $k$  a constant. For massive MIMO systems with  $R \gg 1$  and low correlation between the channels in receiver and transmitter antennas, the elements out of the main diagonal of the matrix, that is,

$$\mathbf{F}_k^H \mathbf{H}_k \quad (10)$$

are much lower than those in the diagonal, where the element  $(i,i)^{\text{th}}$  of the  $\mathbf{F}$  matrix is  $[\mathbf{F}]_{i,i'} = [\mathbf{H}]_{i,i'}$  and  $\mathbf{H}_k$  denotes the  $\mathbf{R} \times \mathbf{T}$  channel matrix for  $k^{\text{th}}$  frequency [19]. Notwithstanding, by employing a frequency-domain receiver with MRC for each frequency, based in  $\mathbf{F}_k^H \mathbf{Y}_k$ , the residual interference levels remains substantial, specially for moderate values of  $\mathbf{R}/\mathbf{T}$ . Therefore and in order to reduce this interference, we propose the interactive receiver depicted in Fig. 3, where

$$\tilde{\mathbf{S}}_k = \Psi \mathbf{F}_k^H \mathbf{Y}_k - \mathbf{B}_k \tilde{\mathbf{S}}_k, \quad (11)$$

with  $\Psi$  denoting the diagonal matrix where the  $(t,t)^{\text{th}}$  element is given by  $(\sum_{k=0}^{N-1} \sum_{r=1}^R |\mathbf{H}_k^{(r,t)}|^2)^{-1}$ . This parameter normalization is appropriate to guarantee that the overall frequency-response of the “channel plus receiver” for each MT has average 1 [9], [11]. The matrix  $\mathbf{B}_k$  is used to reduce the residual ISI and inter-user interference. Clearly, their optimum values are

$$\mathbf{B}_k = \Psi \mathbf{F}_k^H \mathbf{H}_k - \mathbf{I} \quad (12)$$

This cancellation of the interference is made by  $\tilde{\mathbf{S}}_k = [\tilde{S}_0 \dots \tilde{S}_{N-1}]$ , where  $\tilde{\mathbf{S}}_k$  denotes the frequency-domain average values conditioned to the FDE's output at each preceding iteration, which can be computed as referred in [16]. For the first iteration we have not information about the transmitted symbols  $\tilde{\mathbf{S}}_k = 0$ , which means our receiver can be regarded as the simple frequency-domain MRC of the signals associated to different receiver antennas. For the next iteration the average values, conditioned to the receiver output at preceding iteration, will be used to mitigate the residual ISI (Inter-Symbol Interference) and the inter-user interference. In general, for a moderate to high value of SNR (signal-to-noise ratio), the average values conditioned to the receiver output approach the transmitted signals as we increase the number of the iterations, which means that the cancellation of the interference made by  $\mathbf{B}_k$  becomes more efficient and the performance improves. Furthermore, if the average values conditioned to the receiver output can be regarded as “soft decisions” [16], the error propagation effect in our receiver will be significantly reduced.

#### D. EGC-based Iterative Receiver

Within the context of the receivers that don't need matrix inversion operations, we performed the Equal Gain Combining (EGC) of the signals associated to the different receiver antennas. In EGC-based receiver, each signal branch is weighted with the same factor, regardless of the signal amplitude. Moreover, this is simpler to implement than MRC since no controller amplifiers/attenuators and channel estimation are needed. The motivation for this technique lies on the fact that, for a massive MIMO system with  $R \gg 1$ , it can be demonstrated that  $\exp(\mathbf{j} + \arg(\mathbf{H}^H)) \times \mathbf{H} \approx k\mathbf{I}$  with  $k$  designating a constant and  $\mathbf{I}$  a identity matrix. As for MRC, an EGC-based receiver the elements out of the main diagonal of the matrix in  $\mathbf{F}_k^H \mathbf{H}_k$  are much lower than the ones in the diagonal, so the matrix  $\mathbf{F}$  becomes:

$$[\mathbf{F}]_{i,i'} = \exp(\mathbf{j} \arg([\mathbf{H}]_{i,i'})) \quad (13)$$

Once again, we aim to cancel the interference's in the elements out of the main diagonal. For this reason, we implement the iterative EGC receiver depicted in Fig. 3, where the  $\bar{\mathbf{S}}_k$  samples are given by (11) and the new  $\mathbf{B}_k$  by (12). The interference's cancellation is made by the  $\bar{\mathbf{S}}$  coefficients.

#### IV. RESULTS

This section presents a set of performance results concerning the receiver design proposed in this paper. We consider the uplink of a massive MIMO system with  $T = 4$  single-antenna transmitters unless otherwise stated, each one employing an SC-FDE modulation and a receiver with  $R$  antennas. The blocks have  $N = 256$  data symbols, each one selected from a QSPK constellation, plus an appropriate CP. The channel has 100 slots, symbol-spaced, equal-power multipath components, similar conclusions could be drawn for other rich multipath propagation conditions and we consider uncorrelated Rayleigh fading for different multipath components and different links between transmit and receive antennas. We assume perfect synchronization and channel estimation. For the sake of comparison, we also plot the MFB, which can be regarded as a lower bound on the optimum performance [16].

Let us start by comparing conventional ZF, MRC and EGC schemes with the ideal IB-DFE receiver. As expected, the performance of the ZF receiver is acceptable since we are considering  $R > T$ , which reduces the probability of the inverting matrix to be ill conditioned. This would not be the case if  $T = R$ , especially for a small-to-moderate number of antennas. IB-DFE allows an additional gain, leading to a performance very close to the MFB just after a few iterations. In fact, 4 iterations are enough for the convergence of the IB-DFE receiver. However, the low-complexity techniques that do not require matrix inversions (EGC and MRC) have very poor performance, with high irreducible error floors. These error floors decrease as we increase the ratio  $R/T$ , but even for  $R = 32 = 8T$ , receive antennas we still have irreducible error floors in the vicinity of  $10^{-2}$ .

Let us consider now our iterative FDE receivers where the first iteration is based on the MRC and EGC. Fig. 5 and 6 show the corresponding BER performance with different number of iterations. Clearly, our receivers can have excellent performance, even with  $R = 4T = 16$ . In fact, the performance approaches that of to the IB-DFE receiver after just 4 iterations.

It should be pointed out that our iterative receivers do not require matrix inversions and, in spite of that, they can have such a good performance when  $R \gg T$ . Therefore, it would be interesting to evaluate their performance for smaller values of  $R/T$  or smaller values of  $R$  for a given values of  $T$ . The simulation results of this study are shown in Fig. 7. From this figure, we can observe that our EGC or MRC receiver only an option for  $R$  larger than  $T$ , with  $R \geq 2T$ , at least. Even in this case we can have irreducible errors above  $10^{-4}$  for the EGC-based receiver and above  $10^{-3}$  for the MRC-based receiver.

If we compare the performance we can see that the MRC

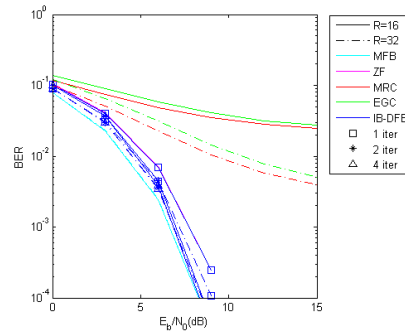


Fig. 4. BER performance for  $T = 4$  and  $R = 16$  or  $32$  receive antennas and an IB-DFE receiver, as well as conventional ZF, EGC and MRC frequency-domain receivers.

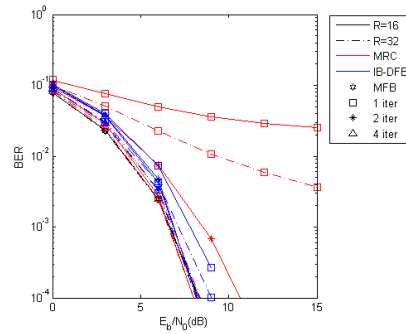


Fig. 5. BER values for  $T = 4$  and  $R = 16$  or  $32$  receiver antennas for the iterative receiver based on the MRC, as well as the IB-DFE receiver.

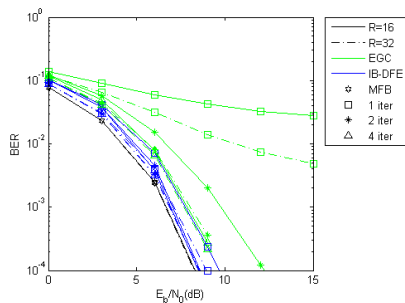


Fig. 6. BER values for  $T = 4$  and  $R = 16$  or  $32$  receiver antennas for the iterative receiver based on the EGC, as well as the IB-DFE receiver.

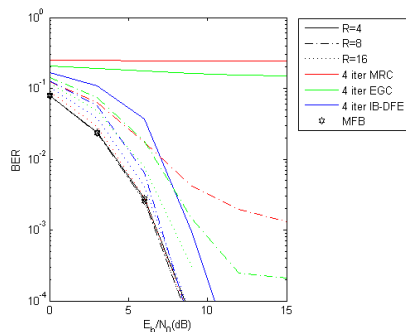


Fig. 7. BER values for  $T = 4$  and different values of  $R$ , with the EGC-based and MRC-based receivers with 4 iterations.

presents a higher performance. This fact is shown in Fig. 7. The simulated results shown in Fig. 5 and 6 show that the EGC approaches the IB-DFE performance while the MRC approaches the MFB.

## V. CONCLUSION

In this paper we considered the uplink of massive MIMO systems employing SC-FDE schemes, where multiple users transmit to a single base station with a large number of antennas. We proposed low-complexity frequency-domain detection schemes based on the MRC or EGC that do not require matrix inversions, while achieving an excellent performance, provided that the number of receiver antennas is at least twice as the number of transmitter ones.

The presented results exhibit an excellent performance at the 4<sup>th</sup> iteration for the MRC and EGC techniques. In fact, we can observe that the 4<sup>th</sup> iteration of the MRC technique already presents a performance very close to the MFB. Moreover, we have shown that this level of performance is achievable without the complexity associated with the inversion of large matrices. Therefore we have demonstrated that massive MIMO can be easily implemented, so it is a promising techniques to be used in future 5G systems.

## ACKNOWLEDGMENT

This work was partially supported by Fundação para a Ciência e Tecnologia (FCT) under the project PEstOE/EEI/LA0008/2013.

## REFERENCES

- [1] J. G. Andrews, *What will 5G be?*, IEEE J. Sel. Areas Commun., vol. 32, no. 6, pp. 1065-1082, 2014.
- [2] Rehman Talukdar and Mridul Saikia, *Evolution and Innovation in 5G Cellular Communication System and Beyond: A Study*, ArXiv e-prints, 2014
- [3] G. J. Foschini, *Layered space-time architecture for wireless communication in a fading enviroment when using multi-element antennas*, Bell Labs Tech. J., vol. 1, no. 2, pp. 41-59, 1996.
- [4] G. Raleigh and J. Cioffi, *Spatio-Temporal Coding for Wireless Communication*, IEEE Trans. on Communications, vol. 46, pp. 357-366, 1998.
- [5] E. G. Larsson, O. Edfors, F. Tufvesson and T. L. Marzetta, *Massive MIMO for next generation wireless systems*, IEEE Communications Magazine, vol. 52, no. 2, pp. 186-195, 2 2014.
- [6] F. Rusek, D. Persson, Buon Kiong Lau, E. G. Larsson, T. L. Marzetta, O. Edfors, and F. Tufvesson, *Scaling Up MIMO: Opportunities and Challenges with Very Large Arrays*, IEEE Signal Processing Magazine, vol. 30, no. 1, pp. 40-60, 1 2013.
- [7] A. Gusmão, R. Dinis, R. Conceição, N. Esteves, *Comparison of two modulation choices for broadband wireless communications*, Proc VTC'00-Spring, vol. 2, pp. 1300-1305, Tokyo, Japan, May 2000
- [8] D. Falconer, S. L. Ariyavisitakul, A. Benyamin-Seeyar and B. Eidson, *Frequency domain equalization for single-carrier broadband wireless systems*, IEEE Communications Magazine, vol. 40, no. 4, pp. 58-66, 2002.
- [9] N. Benvenuto and S. Tomasin, *Block iterative dfe for single carrier modulation*, Electron. Lett., vol. 39, no. 19, pp. 1144-1145, Sep.2002.
- [10] N. Benvenuto, R. Dinis, D. Falconer, and S. Tomasin, *Single carrier modulation with nonlinear frequency domain equalization: An idea whose time has come-again*, Proceedings of the IEEE, vol. 98, no. 1, pp. 69-96, January, 2010.
- [11] R. Dinis, R. Kalbasi, D. Falconer and A. Banihashemi, *Iterative Layered Space-Time Receivers for Single-Carrier Transmission over Severe Time Dispersive Channels*, IEEE Comm. Letters, vol. 8, no. 9, pp. 579-581, Sep. 2004.
- [12] F. Amaral, R. Dinis, P. Montezuma, *Approaching the MFB with Block Transmission Techniques*, European Trans. on Telecommunications, vol. 23, no. 1, pp. 76-86, February, 2012.
- [13] A. Gusmão, P. Torres, R. Dinis, N. Esteves, *A turbo FDE technique for reduced-CP SC-based block transmission systems*. IEEE Trans. Commun. vol. 55, no. 1, pp. 16-20, 2007.
- [14] Fábio José Pinto da Silva, *Frequency-Domain Receiver Design for Doubly-Selective Channel*, July 2015.
- [15] J. Proakis, *Digital Communications*, 4th Edition, McGraw-Hill, 2001.
- [16] P. Silva, R. Dinis, *Frequency-Domain Multiuser Detection for CDMA Systems*, River Publishers, Aalborg, 2012.
- [17] F. Ribeiro, R. Dinis, F. Cercas, A. Silva, *Receiver Design for the Uplink of Base Station Cooperation Systems employing SC-FDE Modulation*, EURASIP Journal on Wireless Communications and Networking, vol. 2015, no. 1, pp. 1-17, January, 2015.
- [18] F. Ribeiro, R. Dinis, F. Cercas, A. Silva, *Analytical performance evaluation of Base Station cooperation systems using SC-FDE modulations with iterative receivers*, Globecom Workshops (GC Wkshps) 2012 IEEE, pp. 637641), Anaheim, USA, 2012
- [19] P. Montezuma and R. Dinis, *Iterative Receiver Based on the EGC for Massive MIMO Schemes using SC-FDE Modulations*. Electronics letters vol. 52, no. 11, pp. 972-974, January 2016.



# Bibliography

- [1] A. Osseiran, F. Boccardi, V. Braun, K. Kusume, P. Marsch, M. Maternia, O. Queseth, M. Schellmann, H. Schotten, H. Taoka, H. Tullberg, M. A. Uusitalo, B. Timus, and M. Fallgren, “Scenarios for 5G mobile and wireless communications: The vision of the METIS project,” *IEEE Communications Magazine*, vol. 52, no. 5, pp. 26–35, 5 2014.
- [2] E. Larsson, O. Edfors, F. Tufvesson, and T. Marzetta, “Massive MIMO for next generation wireless systems,” *IEEE Communications Magazine*, vol. 52, no. 2, pp. 186–195, 2 2014.
- [3] F. Rusek, D. Persson, Buon Kiong Lau, E. G. Larsson, T. L. Marzetta, O. Edfors, and F. Tufvesson, “Scaling Up MIMO: Opportunities and Challenges with Very Large Arrays,” *IEEE Signal Processing Magazine*, vol. 30, no. 1, pp. 40–60, 1 2013.
- [4] N. Benvenuto, R. Dinis, D. Falconer, and S. Tomasin, “Single Carrier Modulation With Nonlinear Frequency Domain Equalization: An Idea Whose Time Has Come - Again,” *Proceedings of the IEEE*, vol. 98, no. 1, pp. 69–96, 1 2010.
- [5] V. Pereira and T. Sousa, “Evolution of Mobile Communications: from 1G to 4G,” *2nd International Working Conference on Performance Modelling and Evaluation of Heterogeneous Networks*, no. July, 2004.
- [6] J. G. Andrews, S. Buzzi, W. Choi, S. V. Hanly, a. Lozano, a. C. K. Soong, and J. C. Zhang, “What Will 5G Be?” *Selected Areas in Communications, IEEE Journal on*, vol. 32, no. 6, pp. 1065–1082, 2014.

- [7] S. Rangan, T. S. Rappaport, and E. Erkip, "Millimeter-wave cellular wireless networks: Potentials and challenges," *Proceedings of the IEEE*, vol. 102, no. 3, pp. 366–385, 2014.
- [8] R. W. Chang, "Synthesis of Band-Limited Orthogonal Signals for Multichannel Data Transmission," *Bell System Technical Journal*, vol. 45, no. 10, pp. 1775–1796, 1966.
- [9] D. Falconer, S. Ariyavisitakul, A. Benyamin-Seeyar, and B. Eidson, "Frequency domain equalization for single-carrier broadband wireless systems," *IEEE Communications Magazine*, vol. 40, no. 4, pp. 58–66, 4 2002.
- [10] L. J. Cimini, "Analysis and Simulation of a Digital Mobile Channel Using Orthogonal Frequency Division Multiplexing," *Communications, IEEE Transactions on*, vol. 33, no. 7, pp. 665–675, 1985.
- [11] M. Gomes, R. Dinis, V. Silva, F. Cercas, and M. Tomlinson, "Error rate analysis of M-PSK with magnitude modulation envelope control," *Electronics Letters*, vol. 49, no. 18, pp. 1184–1186, 2013.
- [12] H. Sari, G. Karam, and I. Jeanclaude, "An analysis of orthogonal frequency-division multiplexing for mobile radio applications," *IEEE 44th Vehicular Technology Conference*, no. m, p. 1635–1639, 1994.
- [13] J. G. Proakis and M. Salehi, *Digital Communications*, 5th ed. McGraw-Hill, 2007.
- [14] A. Gusmão, R. Dinis, J. Conceição, and N. Esteves, "Comparison of two modulation choices for broadband wireless communications," *IEEE 51st Vehicular Technology Conference*, vol. 2, p. 1300–1305, 2000.
- [15] N. Benvenuto and S. Tomasin, "Block iterative DFE for single carrier modulation," *Electronics Letters*, vol. 38, no. 19, pp. 1144–1145, 2002.
- [16] F. Silva, R. Dinis, and P. Montezuma, "Estimation of the Feedback Reliability for IB-DFE Receivers," *ISRN Communications and Networking*, vol. 2011, pp. 1–7, 2011.



- [17] F. Silva, R. Dinis, N. Souto, and P. Montezuma, "Approaching the matched filter bound with block transmission techniques," *Transactions on Emerging Telecommunications Technologies*, vol. 23, no. 1, pp. 76–85, 1 2012.
- [18] G. J. Foschini, "Layered space-time architecture for wireless communication in a fading environment when using multi-element antennas," *Bell Labs Technical Journal*, vol. 1, no. 2, pp. 41–59, 1996.
- [19] M. S. Julius, "MIMO : State of the Art , and the Future in Focus," pp. 1–6.
- [20] P. Bhatnagar, P. M. Tiwari, P. J. Singh, and P. S. Rathore, "Enhancement of OFDM System Performance with MIMO technique," vol. 1, no. 3, pp. 143–146.
- [21] M. S. Osman, H. Y. Soliman, S. M. Abuelenin, and K. S. Al-Barbary, "Performance analysis of a combined STC-SVD MIMO-OFDM system," in *2014 International Conference on Connected Vehicles and Expo (ICCVE)*. IEEE, 11 2014, pp. 1114–1119.
- [22] J. Xuehua and C. Peijiang, "Study and implementation of MIMO-OFDM system based on Matlab," *Proceedings - 2009 International Conference on Information Technology and Computer Science, ITCS 2009*, vol. 1, pp. 554–557, 2009.
- [23] D. W. Browne, M. W. Browne, and M. P. Fitz, "Singular Value Decomposition of Correlated MIMO Channels," in *IEEE Globecom 2006*, vol. 2, no. 2. IEEE, 11 2006, pp. 1–6.
- [24] K. Mitsuyama, T. Kumagai, and N. Iai, "Performance Evaluation of SVD-MIMO-OFDM System with a Thinned-out Number of Precoding Weights," *Antennas and Propagation (ISAP), 2015 International Symposium*, 2015.
- [25] F. Boccardi, R. Heath, A. Lozano, T. Marzetta, and P. Popovski, "Five disruptive technology directions for 5G," *IEEE Communications Magazine*, vol. 52, no. 2, pp. 74–80, 2 2014.

- [26] R. Dinis, R. Kalbasi, D. Falconer, and A. Banihashemi, "Iterative Layered Space-Time Receivers for Single-Carrier Transmission Over Severe Time-Dispersive Channels," *IEEE Communications Letters*, vol. 8, no. 9, pp. 579–581, 9 2004.
- [27] F. C. Ribeiro, R. Dinis, F. Cercas, and A. Silva, "Analytical performance evaluation of Base Station cooperation systems using SC-FDE modulations with iterative receivers," *2012 IEEE Globecom Workshops, GC Wkshps 2012*, pp. 637–641, 2012.
- [28] A. Gusmão, P. Torres, R. Dinis, and N. Esteves, "A turbo FDE technique for reduced-CP SC-based block transmission systems," *IEEE Transactions on Communications*, vol. 55, no. 1, pp. 16–20, 2007.
- [29] F. Ribeiro, R. Dinis, F. Cercas, and A. Silva, "Receiver design for the up-link of base station cooperation systems employing SC-FDE modulations," *EURASIP Journal on Wireless Communications and Networking*, vol. 2015, no. 1, p. 7, 2015.
- [30] R. Dinis, P. Carvalho, and D. Borges, "Low Complexity Mrc and Egc Based Receivers for Sc-Fde Modulations With Massive Mimo Schemes," *IEEE Global Conf. on Signal and Information Processing - Global SIP*, vol. 1, no. 1, pp. 1–4, 2016.
- [31] D.G.BRENNAN, "Linear Diversity Combining Technique," *Proceedings of the IRE*, vol. 10, no. 2, pp. 1075–1102, 1959.
- [32] B. R. Tomiuk and N. C. Beaulieu, "A new look at maximal ratio combining," *Globecom '00 - IEEE. Global Telecommunications Conference. Conference Record (Cat. No.00CH37137)*, vol. 2, no. 613, pp. 943–948, 2000.
- [33] P. Montezuma and R. Dinis, "Iterative receiver based on the EGC for massive MIMO schemes using SC-FDE modulations," *Electronics Letters*, vol. 52, no. 11, pp. 972–974, 5 2016.

- [34] D. Fernandes, F. Cercas, and R. Dinis, “Iterative Receiver Combining IB-DFE with MRC for Massive MIMO Schemes,” *Procedia Computer Science*, vol. 109, pp. 305–310, 2017.